Chromatin protein HMGB2 regulates articular cartilage surface maintenance via β-catenin pathway

Noboru Taniguchi[a], Beatriz Caramés[a], Yasuhiko Kawakami[b], Brad A. Amendt[c], Setsuro Komiya[d], and Martin Lotz[a,1]

[a]Department of Arthritis Research, The Scripps Research Institute, La Jolla, CA 92037; [b]Stem Cell Institute and Department of Genetics, Cell Biology, and Development, University of Minnesota, Minneapolis, MN 55455; [c]Institute of Biosciences and Technology, Texas A&M University System Health Science Center, Houston, TX 77030-3303; and [d]Department of Orthopaedic Surgery, Kagoshima University Graduate School of Medical and Dental Sciences, 8-35-1 Sakuragaoka, Kagoshima 890-8520, Japan

Edited by Peter K. Vogt, The Scripps Research Institute, La Jolla, CA, and approved August 12, 2009 (received for review April 22, 2009)

The superficial zone (SZ) of articular cartilage is critical in maintaining tissue function and homeostasis and represents the site of the earliest changes in osteoarthritis. Mechanisms that regulate the unique phenotype of SZ chondrocytes and maintain SZ integrity are unknown. We recently demonstrated that expression of the chromatin protein high mobility group box (HMGB) protein 2 is restricted to the SZ in articular cartilage suggesting a transcriptional regulation involving HMGB2 in SZ. Here, we show that an interaction between HMGB2 and the Wnt/β-catenin pathway regulates the maintenance of the SZ. We found that the Wnt/β-catenin pathway is active specifically in the SZ in normal mouse knee joints and colocalizes with HMGB2. Both Wnt signaling and HMGB2 expression decrease with aging in mouse joints. Our molecular studies show that HMGB2 enhances the binding of Lef-1 to its target sequence and potentiates transcriptional activation of the Lef-1-β-catenin complex. The HMG domain within HMGB2 is crucial for interaction with Lef-1, suggesting that both HMGB2 and HMGB1 may be involved in this function. Furthermore, conditional deletion of β-catenin in cultured mouse chondrocytes induced apoptosis. These findings define a pathway where protein interactions of HMGB2 and Lef-1 enhance Wnt signaling and promote SZ chondrocyte survival. Loss of the HMGB2-Wnt signaling interaction is a new mechanism in aging-related cartilage pathology.

aging | osteoarthritis | apoptosis | superficial zone

Articular cartilage is a tissue that provides biomechanical properties that allow near frictionless joint movement and dispersion of mechanical loads. Cartilage is composed of a single cell lineage but differences in the organization, phenotype and function of cells in the various layers of cartilage have been recognized (1–4). The superficial zone (SZ) is the most unique. SZ cells produce lubricin, also termed proteoglycan-4 (PRG4) or superficial zone protein (SZP), an important joint lubricant (5–7), and are more responsive to stimulation by catabolic cytokines such as IL-1 (8). Recent studies also suggest that the SZ contains cells that express mesenchymal stem cell markers (9–11).

Articular cartilage is among the tissues that undergo profound aging-related changes and aging represents the major risk factor for osteoarthritis (OA), the most prevalent joint disease (12). Aging-related changes in cartilage include reduced cellularity, increased apoptosis and altered cellular responses to growth factors, cytokines and mechanical stress (13–15). Cartilage changes in aging and OA begin in the SZ and once the SZ is disrupted this is followed by progressive erosion of the remaining cartilage layers (16).

To address mechanisms that maintain the unique phenotype of SZ cells we performed gene expression analyses and observed that expression of the chromatin protein HMGB2 is restricted to the SZ (17). Joint aging in humans and mice leads to loss of HMGB2 expression and this is correlated with the onset of OA-like changes. Mice deficient in *Hmgb2* develop early onset and more severe OA, and this is associated with a reduction in cartilage cellularity attributable to increased cell death (17).

Wnt proteins are secreted factors that regulate cell proliferation and differentiation during early stages of chondrogenesis (18, 19). Overexpression of β-catenin in prechondrogenic cells inhibits overt chondrocytic differentiation (20) and overexpression in chick limb buds accelerates hypertrophic differentiation (21). In contrast, inhibition of β-catenin signaling by overexpression of Frzb-1, dominant negative Wnt receptors, results in delayed maturation (22). Homozygous deletion of β-catenin is embryonic lethal but conditional deletion in cartilage was associated with delayed chondrocyte hypertrophy and reduced chondrocyte proliferation in growth plates (23). Conditional mutant mice deficient in Wnt/β-catenin signaling displayed a defective flat cell layer normally abutting the synovial cavity and markedly reduced levels of PRG4/SZP (24). This supports the importance of Wnt signaling in skeletal development and early stages of chondrocyte differentiation.

Recent studies indicate that Wnt signaling has a role in adult articular cartilage. Increased Wnt signaling due to loss of sFRPS function represents a risk factor for OA (25). Similarly, overexpression of β-catenin in chondrocytes stimulates the expression of matrix degradation enzymes (26). However, Wnt signaling also contributes to differentiation and maintenance of articular cartilage chondrocytes. Inhibition of β-catenin signaling by transgenic overexpression of its intracellular antagonist ICAT results in progressive SZ degradation and development of OA (27). These studies suggest that the precise temporal and spatial activation of Wnt signaling in articular cartilage determines its homeostatic versus pathogenic effects.

Taken together, these reports on Wnt/β-catenin and our observations on HMGB2 suggest possible interactions in the maintenance of the SZ in adult cartilage. Here, we define a molecular mechanism by which HMGB2 and β-catenin regulate cartilage SZ integrity.

Results

β-Catenin Signaling Is Activated in the SZ of Articular Cartilage and Decreases with Aging. β-catenin is an important regulator of chondrocyte maturation in growth plate and its expression and function during skeletal development have been characterized (19, 21, 28). To analyze β-catenin in adult cartilage we used the TOPGAL transgenic mouse model where the β-galactosidase gene is under the control of a LEF/TCF and β-catenin inducible promoter and allows direct detection of cells and tissues with active Wnt signaling (29). Wnt/β-catenin signaling has been reported to be active at early stages during joint formation and to remain active and prominent at later stages in small and large joints (24). In 1-month-old TOPGAL mice, we detected β-galactosidase activity in all zones of articular cartilage. At 3 months with joint maturation it became

Author contributions: N.T. and M.L. designed research; N.T. and B.C. performed research; Y.K. and B.A.A. contributed new reagents/analytic tools; N.T. and M.L. analyzed data; and N.T., S.K., and M.L. wrote the paper.

The authors declare no conflict of interest.

This article is a PNAS Direct Submission.

[1]To whom correspondence should be addressed. E-mail: mlotz@scripps.edu.

This article contains supporting information online at www.pnas.org/cgi/content/full/0904414106/DCSupplemental.

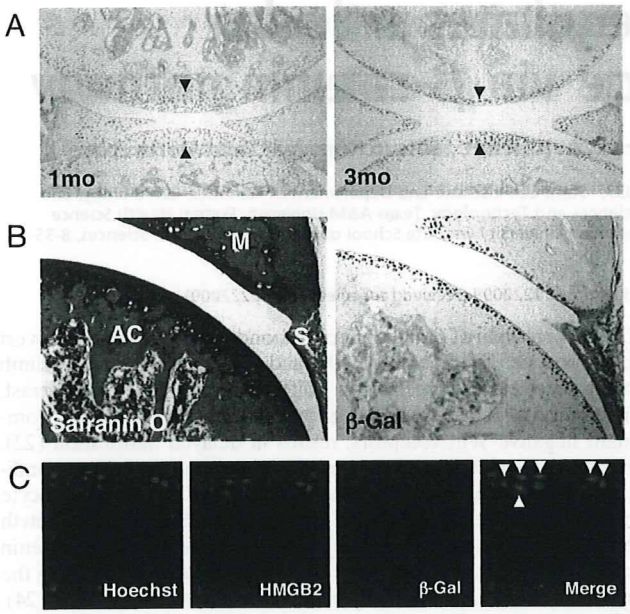

Fig. 1. Active Wnt signaling and correlation with HMGB2 expression in the articular cartilage SZ. (*A*) Immunohistochemistry was performed with β-galactosidase antibody on knee joint sections from 1 and 3-month-old TOPGAL mice. Between 1 and 3 months of age the β-galactosidase positive cells become more restricted to the superficial cell layers in articular cartilage. (*B*) β-galactosidase (β-Gal) positive cells are found in articular cartilage and meniscus, whereas synovium is negative. Safranin O staining of the adjacent section. AC, articular cartilage; M, meniscus; S, synovium. X100. (C) HMGB2 and β-galactosidase expression by immunofluorescence assay. Colocalization of HMGB2 and β-galactosidase (β-Gal) positive cells is found in the SZ in articular cartilage at 3 months of age (arrowheads). Hoechst dye 33258 was used to stain nuclei. (Magnification: ×400.)

more restricted to the cartilage surface (Fig. 1*A*). At this stage, β-galactosidase protein was expressed in the SZ of articular cartilage in meniscus but not in synovium (Fig. 1*B*). Because this pattern is similar to that of HMGB2 (17), we performed double immunofluorescence assay, and verified that most SZ cells express both HMGB2 and β-galactosidase (Fig. 1*C*).

Articular cartilage in C57BL/6J mice undergoes aging-related changes that are similar to osteoarthritis joint pathology (30), and this was also observed in TOPGAL mice on CD1 background (Fig. 2). At 6 months of age articular cartilage had normal appearance, and HMGB2 and β-galactosidase positive cells were present in the superficial cell layers. At 12 months of age there was a reduction in cartilage thickness and cellularity and surface irregularities were prominent in the central weight-bearing areas of the tibial plateau. At 12 months HMGB2 and β-galactosidase were both absent in the SZ in the weight bearing areas, and HMGB2 was completely absent in all regions of articular cartilage by 18 months (Fig. 2). In contrast, β-galactosidase was enhanced in the mid and deep zone, in calcified cartilage, subchondral bone and in osteophytes at 18 months. These findings demonstrate a correlated aging-related loss of HMGB2 and β-catenin signaling in the SZ of articular cartilage and this is associated with OA-like pathology.

Functional Interactions of β-Catenin and HMGB2. The in vivo colocalization of HMGB2 and Wnt/β-catenin activity (Fig. 1) and the correlation of their loss in OA-like pathology suggest interaction of HMGB2 and Wnt/β-catenin in the SZ. To study this in detail, we performed luciferase-reporter assays. Using cyclin D1 promoter (−962CD1) (31), β-catenin transfection caused the expected increase in luciferase activity in both SW1353 chondrosarcoma cells

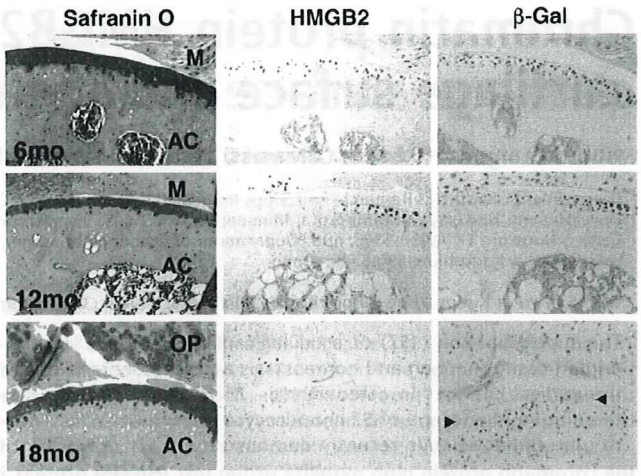

Fig. 2. HMGB2 and β-galactosidase expression during aging in TOPGAL mice. Safranin-O stained sections of joints from TOPGAL mice show normal cartilage at 6 months, reduced thickness and cellularity at 12 and 18 months. HMGB2 and β-galactosidase (β-Gal) are detected by immunohistochemistry at 6 months in the articular cartilage surface. At 12 months both are absent in the weight bearing areas, and HMGB2 is completely absent in the articular cartilage by 18 months. In contrast, at 18 months β-galactosidase becomes detectable in all other zones of articular cartilage except for the SZ (arrowheads). AC, articular cartilage; M, meniscus; OP, osteophyte. X100.

and 293T kidney epithelial cells (Fig. 3 *A* and *B*). Transfection of HMGB2 (32) did not change luciferase activity but cotransfection of HMGB2 and β-catenin resulted in synergistic enhancement in SW1353 chondrosarcoma cells (Fig. 3*A*); this synergy was not observed in 293T kidney epithelial cells (Fig. 3*B*). Similar differences between cell types were obtained using the TOPflash promoter, which contains multiple repeats of the β-catenin-TCF/LEF consensus sequences (33) (Fig. 3 *C* and *D*). The synergistic activity of HMGB2 and β-catenin was also seen in chondrogenic ATDC5 cells. Transfection of the FOPflash promoter with a mutated Lef-1 binding site showed no activity (Fig. 3*E*) but the activity of TOPflash promoter was enhanced by HMGB2 in a dose-dependent manner under β-catenin transfection (Fig. 3*F*). These experiments demonstrate synergistic interaction of β-catenin and HMGB2 in enhancing Lef-1 responsive promoters, specifically in chondrogenic cell types.

Physical Interactions of HMGB2 and Lef-1. To examine molecular interactions between β-catenin, Lef-1 and HMGB2, GST-pull down assays were performed using bacterially expressed GST-HMGB2, β-catenin and Lef-1 and in vitro-translated HMGB2, β catenin and Lef 1 (34). We observed that in vitro translated HMGB2 bound GST-Lef-1, but not GST-β-catenin (Fig. 4*A*). The results from the reverse experiment showed that in vitro-translated Lef-1 interacted with GST-HMGB2 and GST-β-catenin (Fig. 4*B*). When in vitro-translated β-catenin protein was incubated with GST-HMGB2 and GST-Lef-1, only GST-Lef-1 but not GST-HMGB2 was pulled down (Fig. S1). This indicates a specific interaction between HMGB2 and Lef-1, leading to enhanced transcriptional activation of the Lef-1-β-catenin complex.

Interaction Domains of HMGB2 and Lef-1. To define the Lef-1 interaction domain within HMGB2, in vitro GST pull-down assays were performed using GST-Lef-1 and HMGB2 deletion mutants (A-box, B-box, acidic tail) as shown in Fig. S2*A*. The results demonstrated that none of these 3 HMGB2 mutants interacts with Lef-1 (Fig. S2*B*). Then we constructed A-box and B-box domains with linker regions and found that both bind Lef-1 (Fig. S2*B*). Delta box, which contains linker and acidic tail but not A-box or B-box,

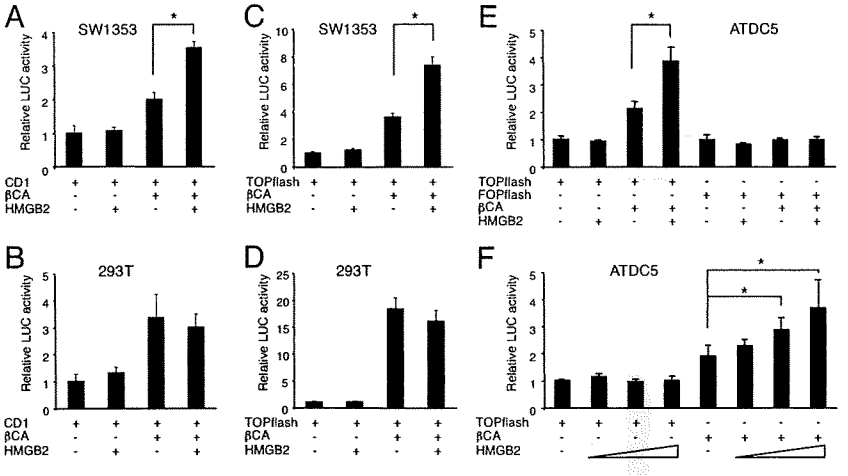

Fig. 3. Synergy of HMGB2 and β-catenin. HMGB2 and β-catenin (βCA) were cotransfected with the cyclin D1 (CD1) (*A* and *B*) and TOPflash reporter genes (*C–F*) in SW1353 cells (*A* and *C*) and 293T cells (*B* and *D*), and luciferase assay was performed after 24 h. In SW1353 cells, HMGB2 enhances luciferase activity when co-transfected with β-catenin (*A* and *C*), whereas this synergistic effect is not seen in 293T cells (*B* and *D*). This synergistic effect is also found with TOPflash in a dose-dependent manner (*F*), but not with FOPflash reporter genes in ATDC5 cells (*E*) (*, $P < 0.05$).

did not interact with Lef-1. These results indicate that A-box or B-box together with the linker region are required for HMGB2 binding to Lef-1.

Next we determined the domains in Lef-1 that are required for interaction with HMGB2. GST pull-down assays were performed with GST-HMGB2 and Lef-1 deletion mutant plasmids (FL, ΔN113, ΔN295, ΔN113-ΔC102) (35). The results showed that GST-HMGB2 could pull down Lef-1 FL (Fig. 4*B*), Lef-1 ΔN113 and Lef-1 ΔN295 but not Lef-1 ΔN113-ΔC102 (Fig. S2*C*), indicating that the HMG domain in Lef-1 is responsible for the physical interaction with HMGB2.

DNA Binding Interactions of HMGB2 and Lef-1. To understand how the HMGB2-Lef-1 interaction contributes to Wnt/β-catenin activity, we examined whether the interaction affects Lef-1 DNA binding. Gel shift assays were performed to determine binding specificity and interactions of HMGB2 and Lef-1. We prepared oligonucleotide probes with Lef-1 binding sites (cyclin D1 and TOP) and a probe with a mutated Lef-1 binding site (FOP) as described in ref. 36. Using nuclear extracts of Lef-1 transfected SW1353 chondrosarcoma cells, we detected binding of Lef-1 to both cyclin D1 and TOP probes, and this binding was enhanced by the addition of purified HMGB2 (Fig. 4*C*). In contrast, no binding was detected on the FOP probe. HMGB2 did not interact with cyclin D1 and TOP probes without overexpressed Lef-1.

c-Jun is a target gene for the β-catenin-Tcf/Lef transcriptional complex (37), and Wnt signaling induces c-Jun expression in chondrocytes (38). We also detected binding of Lef-1 to c-Jun probes in SW1353 cells in the presence of Lef-1, and this binding was potentiated by the addition of HMGB2 protein (Fig. S3). These results suggest that interaction between HMGB2 and Lef-1 enhances DNA binding affinity of Lef-1, to enhance Wnt/β-catenin signaling.

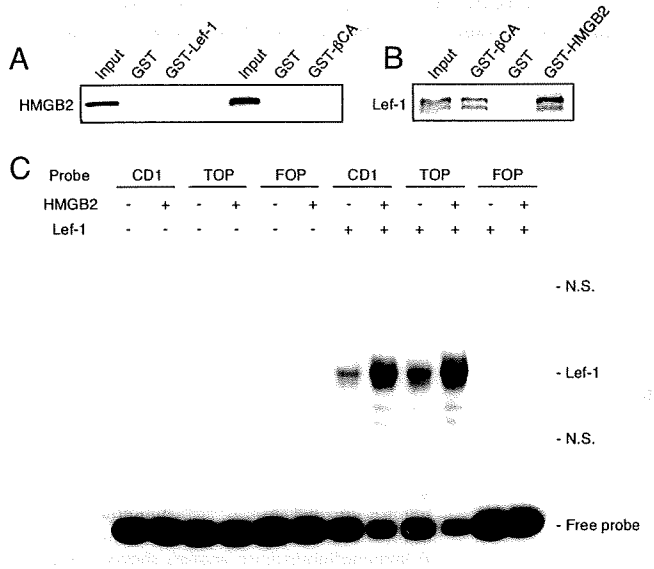

Fig. 4. GST-pull down assay for β-catenin (βCA), Lef-1 and HMGB2. (*A*) In vitro-translated HMGB2 interacts with GST-Lef-1, but not with GST-β-catenin. (*B*) In vitro-translated Lef-1 interacts with both GST-β-catenin and GST-HMGB2. (C) DNA binding interactions of HMGB2 and Lef-1 by EMSA. Using nuclear extracts of SW1353 cells transfected with Lef-1, binding of Lef-1 with both cyclin D1 (CD1) and TOP probes was detected. This was enhanced by the addition of HMGB2 protein (1 μg). In contrast, no binding was detected on the FOP probe. N.S., nonspecific.

HMGB2 and Wnt/β-Catenin Target Gene Expression. To examine whether the interaction between HMGB2 and Lef-1 potentiates Wnt/β-catenin signaling activity, we examined Wnt/β-catenin signaling in WT and *Hmgb2*$^{-/-}$ chondrocytes using SuperTOPflash, which contains 8 TCF/LEF binding sites and the corresponding negative control vector SuperFOPflash (39). We did not detect a difference in luciferase activity between two groups when the cells were unstimulated; however, in response to stimulation with recombinant Wnt3a luciferase activity was increased. Importantly, this activation was significantly lower in *Hmgb2*$^{-/-}$ chondrocytes than in WT chondrocytes (Fig. 5*A*).

To further examine this, we analyzed levels of Wnt/β-catenin targets genes. HMGB2 was reduced by siRNA in immature murine articular chondrocytes, which strongly express endogenous HMGB2 (17) (Fig. 5*B*). Quantitative PCR shows that HMGB2 siRNA reduced cyclin D1 mRNA expression. Additional Wnt/β-catenin target genes, Gli3 and Frizzled 2 (Fzd2), which are expressed in articular cartilage (26, 40), were also reduced by HMGB2 siRNA, whereas PRG4/SZP that is expressed in murine *Hmgb2*$^{-/-}$ chondrocytes and WT chondrocytes was unaffected (17) (Fig. 5*C*).

To verify that HMGB2 does bind to targets of Lef1/β-catenin genes, we used chromatin immunoprecipitation assay. We observed that HMGB2 can facilitate binding affinity of Lef-1 to the human Gli3 enhancer (R2) (Fig. 5 *D* and *E*), which shows strong activity among highly conserved noncoding DNA regions that contained Tcf/Lef binding sequence within human Gli3 locus (R1–4) (41). These results further support our notion that HMGB2 potentiates Wnt/β-catenin activity.

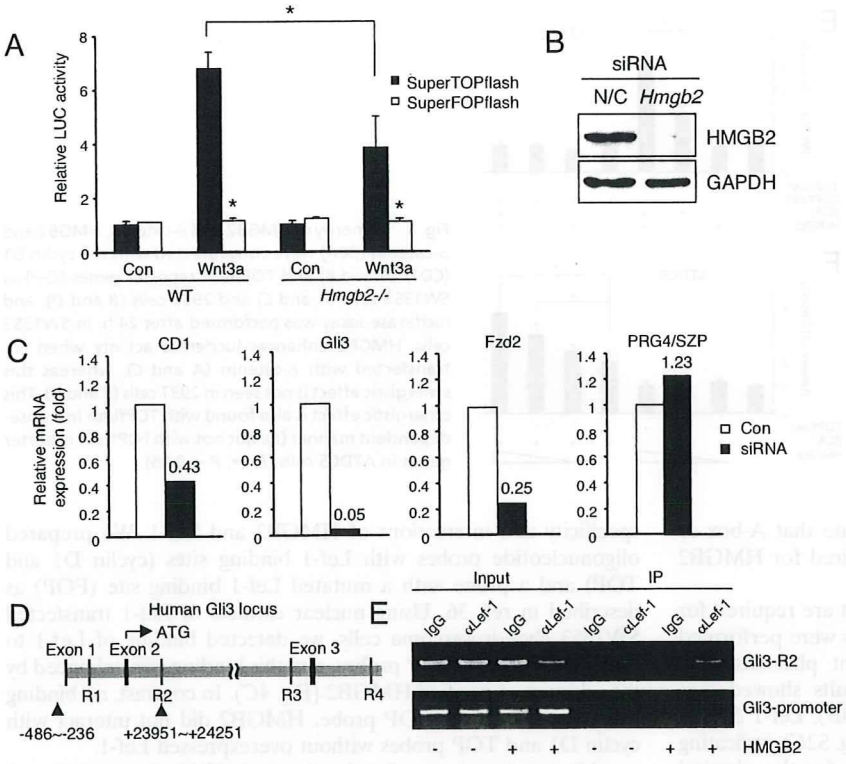

Fig. 5. Wnt/β-catenin signaling in WT and *Hmgb2*$^{-/-}$ chondrocytes. (*A*) SuperTOPflash or SuperFOPflash reporter genes were transfected into murine WT or *Hmgb2*$^{-/-}$ chondrocytes. Upon addition of recombinant Wnt3a, stronger luciferase activity was found in WT chondrocytes compared with *Hmgb2*$^{-/-}$ chondrocytes. SuperFOPflash vector was used as negative control (*, $P < 0.01$). HMGB2 siRNA reduces Wnt/β-catenin target genes in articular chondrocytes. (*B*) Murine chondrocytes were transfected by oligo-siRNA negative control (N/C) or HMGB2 and cultured for 48 h, followed by measurement of HMGB2 by Western blot analysis. HMGB2 siRNA specifically and efficiently down-regulated protein levels of HMGB2. (*C*) mRNA levels of Wnt/β-catenin target genes were measured by real-time PCR. The expression levels of cyclin D1 (CD1), Gli3 and Fzd2 but not PRG4/SZP were reduced in chondrocytes with HMGB2 siRNA. (*D*) Schematic representation of the human GLI3 locus. Gray indicates the Gli3 gene, and Tcf/Lef-binding sites as putative enhancers are depicted in red (R1–4). (*E*) Chromatin immunoprecipitation assay shows that HMGB2 potentiates binding affinity of Lef-1 on human Gli3 enhancer within R2 (*Upper*). Sequences not predicted to contain Tcf/Lef-1 binding sites upstream of the Exon 1 were not pulled down (*Lower*). IP, immunoprecipitation.

Loss of β-Catenin Signaling Results in Chondrocyte Apoptosis. To further test the functional significance of β-catenin signaling we conditionally inactivated β-catenin. Chondrocytes were isolated from knee and hip cartilage of β-catenin floxed mice (Ctnnb1$^{flox/flox}$), infected with adenovirus-GFP-Cre and cultured for 72 h. Immunofluorescence analysis of GFP demonstrated effective adenoviral transduction (Fig. 6*A*). β-catenin protein levels were reduced with increasing amounts of adenovirus-GFP-Cre in Ctnnb1$^{flox/flox}$ chondrocytes (Fig. 6*B*). Next, chondrocytes from Ctnnb1$^{flox/flox}$ mice with or without adenovirus-GFP-Cre infection were analyzed by flow cytometry for viability and the apoptosis marker Annexin V. Upon adenovirus-GFP-Cre infection there was a significant increase in apoptotic cells (Fig. 6*C*) without addition of apoptosis inducers. When the chondrocytes were stimulated with anti-Fas antibody CD95 and proteasome inhibitor MG132 (17), a higher percentage of apoptotic chondrocytes was found after

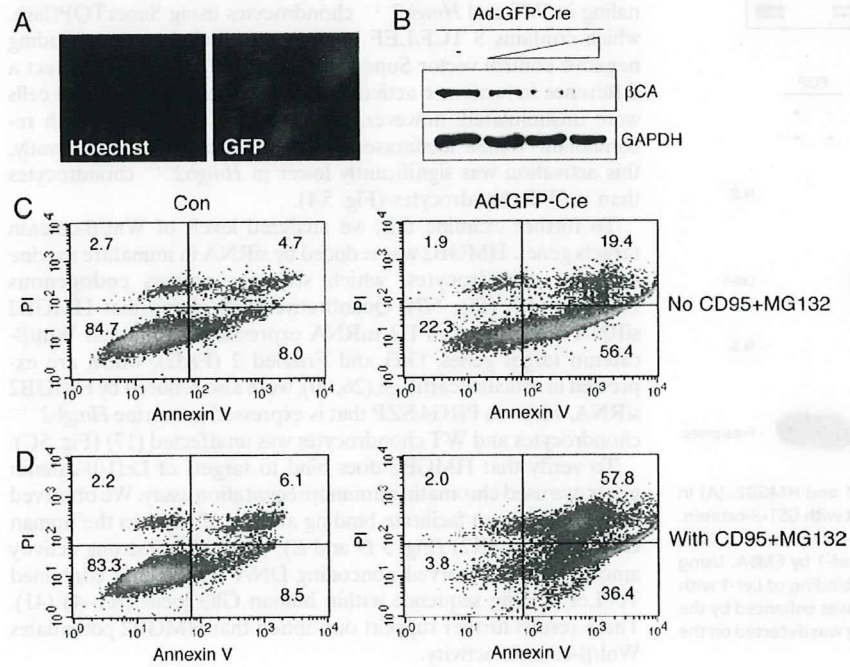

Fig. 6. Conditional inactivation of β-catenin and chondrocyte survival. βCA$^{flox/flox}$ chondrocytes were infected with GFP-Cre adenovirus and cultured for 72 h. (*A*) Immunofluorescence analysis shows GFP expression in infected cells. (*B*) Western blot shows reduction in β-catenin protein levels with increasing amounts of GFP-Cre adenovirus (Ad-GFP-Cre). (*C* and *D*) FACS analysis for annexin V and propidium iodide (PI) staining. GFP-Cre adenovirus infected cultures showed a higher percentage of apoptotic chondrocytes compared with noninfected (Con) cells in the absence or presence of anti-Fas antibody CD95 (1 μg/mL) and MG132 (20 μM).

adenovirus-GFP-Cre infection compared with control (Fig. 6*D*). Thus, β-catenin signaling promotes chondrocyte survival under basal conditions and in response to apoptosis inducers.

Discussion

Understanding mechanisms that control articular cartilage formation and maintenance is of significance to cartilage tissue engineering and the prevention and treatment of diseases affecting articular cartilage. In regards to cartilage tissue engineering a major unmet challenge is the generation of a tissue that recapitulates the zonal organization of normal cartilage. In regards to joint diseases, the major current deficit is in the lack of therapies for OA, the most prevalent form of arthritis. The initial lesions in OA are at the articular surface and once the SZ of cartilage is disrupted, the chronic cartilage remodeling and degradation process is initiated.

To begin elucidating molecular mechanisms that govern the SZ phenotype we showed that the chromatin protein HMGB2 is uniquely expressed in the SZ (17). Aging in humans and mice is associated with a loss of HMGB2 expression, which correlates with OA-like cartilage changes and mice with *Hmgb2* deletion show early onset and more severe OA (17). This observation presented a starting point to further characterize the signaling network in which HMGB2 operates to control SZ cell survival and function.

The Wnt/β-catenin pathway presented a candidate based on a series of recent observations. Most notably, loss of β-catenin signaling leads to OA-like pathology (27). The first observations in this study addressed β-catenin activation patterns in articular cartilage. Wnt/β-catenin signaling is active at multiple embryonic stages of joint formation (24). Postnatally, we observed remarkable similarities between localization of HMGB2 and β-catenin. HMGB2 expression and β-catenin activation were found in all zones of articular cartilage in newborn mice. With joint maturation both became more restricted to the SZ and both showed an aging-related loss in the SZ. Although HMGB2 eventually was completely absent, β-catenin was activated in the other cartilage zones.

To determine molecular mechanisms related to these similarities in expression patterns we analyzed functional and physical interactions. Our EMSA data showed that HMGB2 does not directly bind to regulatory DNA elements but it augments DNA binding of Lef-1. HMGB2 does not alter the electrophoretic mobility of Lef-1 complexed with oligonucleotides, suggesting that HMGB2 dissociates from the complex after having provided its architectural activity (42). Similar results were observed for HMGB1, which increased the affinity of p53 complexes with oligonucleotides (43).

Transfection of HMGB2 did not activate β-catenin responsive promoters but cotransfection of HMGB2 and β-catenin did result in synergistic activation of Lef-1 responsive promoters. This synergy was seen in two chondrogenic cell types, including SW1353 chondrosarcoma cells and ATDC5 prechondrogenic cells but not in lineages such as kidney epithelial cells, suggesting other lineage specific factors mediate this interaction or the difference in both HMGB2 and HMGB1 between chondrogenic cells and 293T cells is responsible (Fig. S4).

Physical interaction studies showed there is no direct binding of HMGB2 and β-catenin. However, HMGB2 binds to Lef-1 and the complex that contains HMGB2, β-catenin, Lef-1 and probably other components leads to enhanced expression of genes containing Lef-1 binding sites. Mapping of interaction domains revealed that the HMG domain in Lef-1 is required for HMGB2 binding. The HMG domain is also responsible for interaction with Notch intracellular domain (44). Notch1 is expressed in developing articular cartilage surface (45) in a pattern similar to HMGB2 (17), indicating that Notch might be involved in Lef1-HMGB2 complex formation in temporally and spatially specific patterns during cartilage formation. HMGB2 has been reported to interact with steroid receptors (46), p53 and p73 (47). Stros et al. reported that B-box within human HMGB1 required the TKKKFKD motif that is included in the linker for interaction with p73, whereas A-box itself can bind p73 (47). It has also been shown that A-box, which contains the linker region within HMGB1, can interact with p53 (48). Our results demonstrate that the A-box or B-box within HMGB2 contribute to binding with Lef-1 only when the linker is present, because A-box, B-box and Δbox deletion mutants did not bind with Lef-1. HMGB1 can also interact with Lef-1 (Fig. S5). Considering that HMGB1 is ubiquitously expressed in the nuclei throughout normal articular cartilage (Fig. S6), we cannot exclude the possibility that HMGB1 and HMGB2 may function cooperatively as coactivators for Wnt/β-catenin signaling in the SZ (17).

The findings on interactions between HMGB2 and the Wnt signaling pathway are similar to a report demonstrating that HMG-17 was responsive to Wnt/β-catenin signaling. HMG-17 forms a chromatin complex with PITX2 to repress PITX2 transcriptional activity. This complex is inactive and switched to an active transcriptional complex through the interaction of β-catenin with PITX2 (49).

To determine functional consequences of the HMGB2/Lef-1 interaction in a cellular context, we analyzed cell survival and expression of representative Lef-1 target genes. The conditional deletion of β-catenin by Cre adenovirus infection of chondrocytes from β-catenin floxed mice increased basal and in vitro induced apoptosis. This observation is consistent with our earlier findings that *Hmgb2* deficient cells are more susceptible to CD95/Fas mediated apoptosis (17). Inhibition of Wnt proteins promotes programmed cell death in different types of cancer cells (50, 51). In human OA cartilage, FrzB-2 is highly expressed and is associated with chondrocyte apoptosis (52). In Col2a1-ICAT-transgenic mice in which β-catenin signaling is selectively blocked in chondrocytes, apoptosis is increased (27).

Our results also show that promoters with Lef-1 binding sites were less responsive to Wnt3a treatment in *Hmgb2*$^{-/-}$ chondrocytes compared with WT chondrocytes. Then we analyzed cyclin D1, Gli3 and Fzd2, three representative and well characterized Lef-1 target genes in cartilage (26, 40, 53). The expression levels of these genes were reduced by HMGB2 siRNA in chondrocytes. Thus, it is possible that reduction of these three genes at least in part explains the increased apoptosis seen in both the *Hmgb2* deficient mice (17) and in chondrocytes with deficient β-catenin (27).

In conclusion, this study demonstrates similar expression and activation patterns of HMGB2 and β-catenin in articular cartilage and that a loss of these pathways in the SZ of articular cartilage may lead to altered gene expression, cell death and OA-like changes.

Materials and Methods

Mice. The β-catenin floxed mice (β-catenin$^{flox/flox}$) with loxP sites in introns 1 and 6 of the β-catenin gene (6.129-Ctnnb1tmKem/KnwJ line) and TOPGAL mice (Tg(Fos-lacZ)34Efu/J line) (29) were purchased from the Jackson Laboratory. Mice were used according to protocols approved by the Institutional Animal Care and Use Committee at The Scripps Research Institute.

Plasmid Construction. The HMGB2 deletion constructs were prepared by PCR amplification of full-length murine HMGB2 cDNA and cloned into pcDNA3-flag vector after the mapping of A-box and B-box within human HMGB2 (54). pGEX-HMGB2 and pGEX-HMGB1 were constructed by subcloning of murine HMGB2 or human HMGB1 into pGEX (Promega), respectively. pGEX-β-catenin was provided by X. He (Harvard Medical School, Boston) and pGEX-Lef-1 by M.R. Stallcup (University of Southern California, Los Angeles).

GST Pull-Down Assay. The wild-type and deletion mutants of HMGB2 and Lef-1 were in vitro transcribed/translated with the TNT reticulocyte lysate kit (Promega) in the presence of [^{35}S]methionine. GST-null, GST-HMGB2, GST-Lef-1, or GST-β-catenin proteins were produced in *E. coli* and purified, and then incubated overnight at 4 °C rotating with the ^{35}S-met-labeled proteins in PC100+βME buffer (55). After extensive washes, we added SDS loading buffer to the beads, boiled them, and separated the supernatant on SDS/PAGE gels. As a positive control, the amount of ^{35}S-met-labeled protein loaded was 20% of the input. The gels were dried and then exposed to X-ray film.

Electrophoretic Mobility-Shift Assay (EMSA). Preparation of DNA for EMSA with ^{32}P-labeled duplex oligonucleotide probes for CD1, CD1TOP and CD1FOP was described earlier (36). We also generated synthetic duplex oligonucleotides encompassing regions evolutionarily conserved in the c-Jun promoter (37). The binding reaction contained 40,000 cpm of ^{32}P-labeled DNA that was incubated with nuclear extracts from SW1353 cells with or without transfection of HA-tagged Lef-1 expression vector (gift from P.K. Vogt, The Scripps Research Institute) in the presence of purified calf thymus HMGB2 protein (Shino-Test), following Gel Shift Assay Systems Protocol (Promega). DNA-protein complexes were electrophoresed in 6% DNA retardation gel (Invitrogen) and visualized by autoradiography.

Quantitative PCR. Total RNA was extracted and oligo(dT)-primed cDNA was prepared from 500 ng of total RNA by using SuperScript III (Invitrogen). The resulting cDNAs were analyzed by using the SYBR green system for quantitative analysis of specific transcripts as described in ref. 56. All mRNA expression data were normalized to GAPDH expression in the same sample. The primers used in real-time PCR are listed in *SI Text*.

Apoptosis Induction and Analysis in Vitro. Chondrocytes were prepared from 5-day-old β-catenin floxed mice (β-catenin$^{flox/flox}$) as described in ref. 57. The cells were plated in 6-well plates at semiconfluence, infected with adenovirus expressing both Cre recombinase and green fluorescent protein (GFP) (Adv-Cre-GFP) and cultured for 72 h. We used an E1/E3-deleted, replication-incompetent, serotype 5 adenovirus-expressing Cre recombinase and GFP under control of the cytomegalovirus (CMV) promoter. Medium was changed to DMEM/F12 with 0.5% FBS and chondrocytes were stimulated with NA/LE hamster anti-mouse CD95 antibody (BD PharMingen) and proteasome inhibitor MG132 (Sigma) for 12 h, which induces apoptosis in articular chondrocytes (58). Cells were incubated with FITC-labeled annexin V (BD PharMingen) or propidium iodide (Sigma) and analyzed on a BD FACSCalibur as described in ref. 17.

Statistical Analysis. Results are expressed as mean ± standard deviation. Statistical comparison between genotypes or treatment groups was performed with a two-tailed Student's *t* test. *P* values <0.05 were considered significant.

ACKNOWLEDGMENTS. We thank Lilo Creighton, Jean Valbracht and Diana Brinson for technical support and Marco E. Bianchi (San Raffaele University, Milan, Italy) for helpful discussions. This work was supported by National Institutes of Health Grants AG007996 and AG033409 (to M.L.), the Arthritis National Research Foundation and Japan Orthopaedics and Traumatology Foundation, Inc. No. 179 (to N.T.), and the Sam and Rose Stein Endowment Fund (M.L.).

1. Korver GH, van de Stadt RJ, van Kampen GP, van der Korst JK (1990) Composition of proteoglycans synthesized in different layers of cultured anatomically intact articular cartilage. *Matrix* 10:394–401.
2. Hunziker EB, Quinn TM, Hauselmann HJ (2002) Quantitative structural organization of normal adult human articular cartilage. *Osteoarthritis Cartilage* 10:564–572.
3. Darling EM, Hu JC, Athanasiou KA (2004) Zonal and topographical differences in articular cartilage gene expression. *J Orthop Res* 22:1182–1187.
4. Aydelotte MB, Kuettner KE (1988) Differences between sub-populations of cultured bovine articular chondrocytes. I. Morphology and cartilage matrix production. *Connect Tissue Res* 18:205–222.
5. Flannery CR, et al. (1999) Articular cartilage superficial zone protein (SZP) is homologous to megakaryocyte stimulating factor precursor and Is a multifunctional proteoglycan with potential growth-promoting, cytoprotective, and lubricating properties in cartilage metabolism. *Biochem Biophys Res Commun* 254:535–541.
6. Rhee DK, et al. (2005) The secreted glycoprotein lubricin protects cartilage surfaces and inhibits synovial cell overgrowth. *J Clin Invest* 115:622–631.
7. Schumacher BL, Hughes CE, Kuettner KE, Caterson B, Aydelotte MB (1999) Immunodetection and partial cDNA sequence of the proteoglycan, superficial zone protein, synthesized by cells lining synovial joints. *J Orthop Res* 17:110–120.
8. Hauselmann HJ, Stefanovic-Racic M, Michel BA, Evans CH (1998) Differences in nitric oxide production by superficial and deep human articular chondrocytes: Implications for proteoglycan turnover in inflammatory joint diseases. *J Immunol* 160:1444–1448.
9. Hiraoka K, Grogan S, Olee T, Lotz M Mesenchymal progenitor cells in adult human articular cartilage. *Biorheology* 43(3–4):447–454, 2006.
10. Alsalameh S, Amin R, Gemba T, Lotz M (2004) Identification of mesenchymal progenitor cells in normal and osteoarthritic human articular cartilage. *Arthritis Rheum* 50:1522–1532.
11. Dowthwaite GP, et al. (2004) The surface of articular cartilage contains a progenitor cell population. *J Cell Sci* 117(Pt 6):889–897.
12. Bierma-Zeinstra SM, Koes BW (2007) Risk factors and prognostic factors of hip and knee osteoarthritis. *Nat Clin Pract Rheumatol* 3:78–85.
13. Goldring MB (2000) The role of the chondrocyte in osteoarthritis. *Arthritis Rheum* 43:1916–1926.
14. Kuhn K, D'Lima DD, Hashimoto S, Lotz M (2004) Cell death in cartilage. *Osteoarthritis Cartilage* 12:1–16.
15. Abramson SB (2004) Inflammation in osteoarthritis. *J Rheumatol Suppl* 70:70–76.
16. Poole AR, Guilak F, Abramson S (2007) Etiopathogenesis of osteoarthritis. *Osteoarthritis*, ed Moskowitz R (Wolters Kluwer, Philadelphia).
17. Taniguchi N, et al. (2009) Aging-related loss of the chromatin protein HMGB2 in articular cartilage is linked to reduced cellularity and osteoarthritis. *Proc Natl Acad Sci USA* 106:1181–1186.
18. Johnson ML, Kamel MA (2007) The Wnt signaling pathway and bone metabolism. *Curr Opin Rheumatol* 19:376–382.
19. Goldring SR, Goldring MB (2007) Eating bone or adding it: The Wnt pathway decides. *Nat Med* 13:133–134.
20. Ryu JH, Chun JS (2006) Opposing roles of WNT-5A and WNT-11 in interleukin-1β regulation of type II collagen expression in articular chondrocytes. *J Biol Chem* 281:22039–22047.
21. Hartmann C, Tabin CJ (2000) Dual roles of Wnt signaling during chondrogenesis in the chicken limb. *Development* 127:3141–3159.
22. Enomoto-Iwamoto M, et al. (2002) The Wnt antagonist Frzb-1 regulates chondrocyte maturation and long bone development during limb skeletogenesis. *Dev Biol* 251:142–156.
23. Day TF, Guo X, Garrett-Beal L, Yang Y (2005) Wnt/β-catenin signaling in mesenchymal progenitors controls osteoblast and chondrocyte differentiation during vertebrate skeletogenesis. *Dev Cell* 8:739–750.
24. Koyama E, et al. (2008) A distinct cohort of progenitor cells participates in synovial joint and articular cartilage formation during mouse limb skeletogenesis. *Dev Biol* 316:62–73.
25. Loughlin J, et al. (2004) Functional variants within the secreted frizzled-related protein 3 gene are associated with hip osteoarthritis in females. *Proc Natl Acad Sci USA* 101:9757–9762.
26. Tamamura Y, et al. (2005) Developmental regulation of Wnt/β-catenin signals is required for growth plate assembly, cartilage integrity, and endochondral ossification. *J Biol Chem* 280:19185–19195.
27. Zhu M, et al. (2008) Inhibition of β-catenin signaling in articular chondrocytes results in articular cartilage destruction. *Arthritis Rheum* 58:2053–2064.
28. Guo X, et al. (2004) Wnt/β-catenin signaling is sufficient and necessary for synovial joint formation. *Genes Dev* 18:2404–2417.
29. DasGupta R, Fuchs E (1999) Multiple roles for activated LEF/TCF transcription complexes during hair follicle development and differentiation. *Development* 126:4557–4568.
30. Stanescu R, Knyszynski A, Muriel MP, Stanescu V (1993) Early lesions of the articular surface in a strain of mice with very high incidence of spontaneous osteoarthritic-like lesions. *J Rheumatol* 20:102–110.
31. Tetsu O, McCormick F (1999) Beta-catenin regulates expression of cyclin D1 in colon carcinoma cells. *Nature* 398:422–426.
32. Ronfani L, et al. (2001) Reduced fertility and spermatogenesis defects in mice lacking chromosomal protein Hmgb2. *Development* 128:1265–1273.
33. Korinek V, et al. (1997) Constitutive transcriptional activation by a β-catenin-Tcf complex in APC$^{-/-}$ colon carcinoma. *Science* 275:1784–1787.
34. Kawakami Y, et al. (2005) Transcriptional coactivator PGC-1α regulates chondrogenesis via association with Sox9. *Proc Natl Acad Sci USA* 102:2414–2419.
35. Diamond E, Amen M, Hu Q, Espinoza HM, Amendt BA (2006) Functional interactions between Dlx2 and lymphoid enhancer factor regulate Msx2. *Nucleic Acids Res* 34:5951–5965.
36. Shtutman M, et al. (1999) The cyclin D1 gene is a target of the β-catenin/LEF-1 pathway. *Proc Natl Acad Sci USA* 96:5522–5527.
37. Mann B, et al. (1999) Target genes of β-catenin-T cell-factor/lymphoid-enhancer-factor signaling in human colorectal carcinomas. *Proc Natl Acad Sci USA* 96:1603–1608.
38. Hwang SG, Yu SS, Lee SW, Chun JS (2005) Wnt-3a regulates chondrocyte differentiation via c-Jun/AP-1 pathway. *FEBS Lett* 579:4837–4842.
39. Veeman MT, Slusarski DC, Kaykas A, Louie SH, Moon RT (2003) Zebrafish prickle, a modulator of noncanonical Wnt/Fz signaling, regulates gastrulation movements. *Curr Biol* 13:680–685.
40. Robinson JA, et al. (2006) Wnt/β-catenin signaling is a normal physiological response to mechanical loading in bone. *J Biol Chem* 281:31720–31728.
41. Alvarez-Medina R, Cayuso J, Okubo T, Takada S, Marti E (2008) Wnt canonical pathway restricts graded Shh/Gli patterning activity through the regulation of Gli3 expression. *Development* 135:237–247.
42. Agresti A, Bianchi ME (2003) HMGB proteins and gene expression. *Curr Opin Genet Dev* 13:170–178.
43. Jayaraman L, et al. (1998) High mobility group protein-1 (HMG-1) is a unique activator of p53. *Genes Dev* 12:462–472.
44. Ross DA, Kadesch T (2001) The notch intracellular domain can function as a coactivator for LEF-1. *Mol Cell Biol* 21:7537–7544.
45. Hayes AJ, Dowthwaite GP, Webster SV, Archer CW (2003) The distribution of Notch receptors and their ligands during articular cartilage development. *J Anat* 202:495–502.
46. Boonyaratanakornkit V, et al. (1998) High-mobility group chromatin proteins 1 and 2 functionally interact with steroid hormone receptors to enhance their DNA binding in vitro and transcriptional activity in mammalian cells. *Mol Cell Biol* 18:4471–4487.
47. Stros M, Ozaki T, Bacikova A, Kageyama H, Nakagawara A (2002) HMGB1 and HMGB2 cell-specifically down-regulate the p53- and p73-dependent sequence-specific transactivation from the human Bax gene promoter. *J Biol Chem* 277:7157–7164.
48. Imamura T, et al. (2001) Interaction with p53 enhances binding of cisplatin-modified DNA by high mobility group 1 protein. *J Biol Chem* 276:7534–7540.
49. Amen M, et al. (2008) Chromatin-associated HMG-17 is a major regulator of homeodomain transcription factor activity modulated by Wnt/β-catenin signaling. *Nucleic Acids Res* 36:462–476.
50. He B, et al. (2005) Blockade of Wnt-1 signaling induces apoptosis in human colorectal cancer cells containing downstream mutations. *Oncogene* 24:3054–3058.
51. You L, et al. (2004) An anti-Wnt-2 monoclonal antibody induces apoptosis in malignant melanoma cells and inhibits tumor growth. *Cancer Res* 64:5385–5389.
52. James IE, et al. (2000) FrzB-2: A human secreted frizzled-related protein with a potential role in chondrocyte apoptosis. *Osteoarthritis Cartilage* 8:452–463.
53. Akiyama H, et al. (2004) Interactions between Sox9 and β-catenin control chondrocyte differentiation. *Genes Dev* 18:1072–1087.
54. Vaccari T, Beltrame M, Ferrari S, Bianchi ME (1998) Hmg4, a new member of the Hmg1/2 gene family. *Genomics* 49:247–252.
55. Tsuda M, Takahashi S, Takahashi Y, Asahara H (2003) Transcriptional co-activators CREB-binding protein and p300 regulate chondrocyte-specific gene expression via association with Sox9. *J Biol Chem* 278:27224–27229.
56. Taniguchi N, et al. (2007) Stage-specific secretion of HMGB1 in cartilage regulates endochondral ossification. *Mol Cell Biol* 27:5650–5663.
57. Salvat C, Pigenet A, Humbert L, Berenbaum F, Thirion S (2005) Immature murine articular chondrocytes in primary culture: A new tool for investigating cartilage. *Osteoarthritis Cartilage* 13:243–249.
58. Kuhn K, Lotz M (2001) Regulation of CD95 (Fas/APO-1)-induced apoptosis in human chondrocytes. *Arthritis Rheum* 44:1644–1653.

Laboratory Investigation (2009) 89, 278–289

Intraocular expression and release of high-mobility group box 1 protein in retinal detachment

Noboru Arimura[1,2], Yuya Ki-i[1,2], Teruto Hashiguchi[2], Ko-ichi Kawahara[2], Kamal K Biswas[2], Makoto Nakamura[3], Yasushi Sonoda[1], Keita Yamakiri[1], Akiko Okubo[1], Taiji Sakamoto[1] and Ikuro Maruyama[2]

High-mobility group box 1 (HMGB1) protein is a multifunctional protein, which is mainly present in the nucleus and is released extracellularly by dying cells and/or activated immune cells. Although extracellular HMGB1 is thought to be a typical danger signal of tissue damage and is implicated in diverse diseases, its relevance to ocular diseases is mostly unknown. To determine whether HMGB1 contributes to the pathogenesis of retinal detachment (RD), which involves photoreceptor degeneration, we investigated the expression and release of HMGB1 both in a retinal cell death induced by excessive oxidative stress *in vitro* and in a rat model of RD-induced photoreceptor degeneration *in vivo*. In addition, we assessed the vitreous concentrations of HMGB1 and monocyte chemoattractant protein 1 (MCP-1) in human eyes with RD. We also explored the chemotactic activity of recombinant HMGB1 in a human retinal pigment epithelial (RPE) cell line. The results show that the nuclear HMGB1 in the retinal cell is augmented by death stress and upregulation appears to be required for cell survival, whereas extracellular release of HMGB1 is evident not only in retinal cell death *in vitro* but also in the rat model of RD *in vivo*. Furthermore, the vitreous level of HMGB1 is significantly increased and is correlated with that of MCP-1 in human eyes with RD. Recombinant HMGB1 induced RPE cell migration through an extracellular signal-regulated kinase-dependent mechanism *in vitro*. Our findings suggest that HMGB1 is a crucial nuclear protein and is released as a danger signal of retinal tissue damage. Extracellular HMGB1 might be an important mediator in RD, potentially acting as a chemotactic factor for RPE cell migration that would lead to an ocular pathological wound-healing response.

Laboratory Investigation (2009) **89,** 278–289; doi:10.1038/labinvest.2008.165; published online 12 January 2009

KEYWORDS: danger signal; high-mobility group box 1 protein; photoreceptor degeneration; retinal detachment; tissue damage; wound healing

Cell death is the predominant event of degenerative tissue damage and can be a trigger that activates the immune system and repair program. Recently, there has been much interest in the pivotal role of endogenous danger signals released during cell death.[1] High-mobility group box 1 (HMGB1) protein is a prototypic innate danger signal, and appears to be crucial in this context because extracellular HMGB1 [2] can modulate inflammation, proliferation, and remodeling, which are involved in the wound-healing process.[3]

HMGB1 was originally described as an abundant and ubiquitous nuclear DNA-binding protein that had multiple functions dependent on its cellular location.[2,4] In the nucleus, HMGB1 binds to DNA and is critical for proper transcriptional regulation. It is also called amphoterin and accelerates cellular motility on the cell surface.[5] HMGB1 is reported to be passively released into the extracellular milieu by necrotic cells, but not by apoptotic cells,[6] or is exported actively by monocytes/macrophages[7] and neural cells[8] upon receiving appropriate stimuli. In damaged tissue, extracellular HMGB1 acts as a necrotic signal, which alerts the surrounding cells and the immune system.[2] Although extracellular HMGB1 can contribute to normal tissue development and repair, it is also implicated in the pathogenesis of several diseases (including lethal endotoxemia,[7] disseminated intravascular coagulation,[9] ischemic brain,[10] tumor,[11] atherosclerosis,[12] rheumatoid arthritis,[13] and periodontitis[14]).

[1]Department of Ophthalmology, Kagoshima University Graduate School of Medical and Dental Sciences, Kagoshima, Japan; [2]Department of Laboratory and Vascular Medicine, Kagoshima University Graduate School of Medical and Dental Sciences, Kagoshima, Japan and [3]Division of Ophthalmology, Department of Surgery, Kobe University Graduate School of Medicine, Kobe, Japan
Correspondence: Professor T Sakamoto, MD, PhD, Department of Ophthalmology, Kagoshima University Graduate School of Medical and Dental Sciences, 8-35-1, Sakuragaoka, Kagoshima 890-8520, Japan.
E-mail: tsakamot@m3.kufm.kagoshima-u.ac.jp

Received 25 August 2008; revised 9 October 2008; accepted 13 October 2008

Retinal detachment (RD), the physical separation of photoreceptors from the underlying retinal pigment epithelium (RPE), is one of the main causes of visual loss. Photoreceptor degeneration due to RD is thought to be executed by apoptosis[15,16] and necrosis,[17] which usually occur after tissue damage. Although retinal cell death and the following reactive responses must occur in almost all forms of retinal disease including RD,[18] data regarding the relationship among cell death, danger, and responses in the eye, have been very limited, especially in terms of danger signals. We previously reported that HMGB1 was significantly elevated in inflamed eyes with endophthalmitis, and suggested a possible link between HMGB1 and ocular inflammatory diseases.[19] On the other hand, considering the properties of HMGB1, we hypothesized that HMGB1 might have some roles in photoreceptor degeneration and subsequent damage-associated reactions in RD.

To investigate whether HMGB1 is involved in the pathogenesis of RD, we first examined the expression and release of HMGB1 both in a retinal cell death *in vitro* and in a rat model of RD-induced photoreceptor degeneration *in vivo*. To focus on human RD, we assessed the intravitreous concentrations of HMGB1 in human eyes affected by RD. Monocyte chemoattractant protein 1 (MCP-1), which was recently documented to be a potential proapoptotic mediator in RD,[20] was also measured in the same vitreous samples. We further analyzed the effects of recombinant HMGB1 (rHMGB1) on chemotactic activity in a RPE cell line *in vitro*. Our findings suggest that extracellular HMGB1 is evident in eyes with RD as a danger signal, potentially acting as a chemotactic factor for RPE cell migration that would lead to ocular pathological wound healing.

MATERIALS AND METHODS

Reagents

Full-length, LPS-free rat rHMGB1 protein, which is 99% identical to human HMGB1 and is fully functional on cells of mammalian origin,[21] was purchased from HMGBiotech (Milan, Italy). Human recombinant MCP-1 (rMCP-1) was purchased from Peprotec (Rocky Hill, NJ). Rabbit polyclonal antibody against HMGB1 was provided by Shino-Test Corporation (Kanagawa, Japan). Antibodies against phospho- and total extracellular signal-regulated kinase (ERK)-1/2 were obtained from Cell Signaling Technology (Beverly, MA). U0126 was obtained from Calbiochem (La Jolla, CA).

Human Vitreous Samples

This study was approved by our institutional ethical committee (Kagoshima University Hospital), and was performed in accordance with the Declaration of Helsinki. All surgeries were performed at Kagoshima University Hospital. All patients gave informed consent before treatment. The clinical histories of all patients were obtained from their medical records. Undiluted vitreous fluid samples (0.5–0.7 ml) were obtained by pars plana vitrectomy. Vitreous humor was collected in sterile tubes, placed immediately on ice, centrifuged to remove cells and debris, and stored at −80°C until analysis.

Animals

All animal experiments were performed in accordance with the Association for Research in Vision and Ophthalmology Statement for the Use of Animals in Ophthalmic and Visual Research and the approval of our institutional animal care committee (Kagoshima University). Adult male Brown Norway rats (250–300 g; KBT Oriental, Saga, Japan) were housed in covered cages and kept at constant temperature and relative humidity with a regular 12-h light–dark schedule. Food and water were available *ad libitum*.

Surgical Induction of RD

Rat experimental RD was induced as described previously.[22] Briefly, the rats were anesthetized with an intramuscular injection of ketamine and xylazine, and their pupils were dilated with topical 1% tropicamide and 2.5% phenylephrine hydrochloride. The retinas were detached using a subretinal injection of 1% sodium hyaluronate (Opegan; Santen, Osaka, Japan) with an anterior chamber puncture to reduce intraocular pressure. Sodium hyaluronate (0.05 ml) was slowly injected through the sclera into the subretinal space to enlarge the RDs. These procedures were performed only in the right eye, with the left eye serving as a control. Eyes with lens injury, vitreous hemorrhage, infection, and spontaneous reattachment were excluded from the following analysis. The rats were killed at 3, 7, and 14 days after treatment, with six animals per each time point.

Cell Culture

The rat immortalized retinal precursor cell line R28, a kind gift from Dr GM Siegel (The State University of New York, Buffalo), was cultured in Dulbecco's modified Eagle's medium (DMEM) high glucose supplemented with 10% fetal bovine serum (FBS), 10 mM non-essential amino acids, and 10 μg/ml gentamicin as described previously.[23] The human immortalized RPE cell line ARPE-19, obtained from American Type Culture Collection (Manassas, VA), was grown in DMEM/F12 supplemented with 10% FBS, 2% penicillin–streptomycin, and 1% fungizone (all products were obtained from Invitrogen-Gibco, Rockville, MD). Cells were incubated at 37°C in a 5% CO_2 incubator and subcultured with 0.05% trypsin-EDTA. Subconfluent cultures were trypsinized and seeded for the following experiments. ARPE-19 cells were obtained at passage 21 and used at passages 24–30. Increased passage did not alter the following experimental results up to this passage number.

Cell Viability Assay

Cell viability was analyzed by mitochondrial respiratory activity measured using MTT (3-(4,5-dimethylthiazol-2yl)-2,5-diphenol tetrazolium bromide) assay (Wako Chemicals,

Osaka, Japan), as described previously.[24] Briefly, 2×10^5 R28 cells were cultured in 24-well plates (500 μl medium per well) with or without hydrogen peroxide (1 mM; Merck, Darmstadt, Germany) for 24 h. Then the cells were incubated with MTT (0.5 mg/ml; final concentration) for 3 h. Formazan product was solubilized by the addition of dimethyl sulfoxide for 16 h. Dehydrogenase activity was expressed as absorbance at a test wavelength of 570 nm and at a reference wavelength of 630 nm. Assays were performed in triplicate and repeated three times in independent experiments.

Immunofluorescence for HMGB1 and TUNEL

Indirect immunofluorescence was carried out as described previously,[19,25] with some modifications. The eyes were harvested and fixed in 4% paraformaldehyde at 4°C overnight. The anterior segment and the lens were removed, and the remaining eye cup was cryoprotected with 10–30% sucrose in phosphate-buffered saline. The eye cups were then frozen in an optimal cutting temperature compound (Sakura Finetech, Tokyo, Japan). Sections were cut at 8 μm with a cryostat (Leica Microsystems, Wetzler, Germany). After being incubated with blocking buffer containing 10% goat serum, 1% bovine serum albumin (BSA), and 0.05% Tween-20 for 1 h, the slides were incubated with rabbit polyclonal anti-HMGB1 antibody (1 μg/ml). After overnight incubation, sections were washed and probed with Alexa-Fluor 594-conjugated goat anti-rabbit IgG F(ab')2 fragment (Molecular Probes, Carlsbad, CA) for 1 h. In some experiments, TUNEL co-staining was also performed according to the manufacturer's protocol (ApopTag Fluorescein *In situ* Apoptosis Detection kit; Chemicon, Temecula, CA) as previously described.[22] Slides were counterstained with DAPI, mounted with Shandon PermaFlour (Thermo Scientific, Waltham, MA), and viewed with a Zeiss fluorescence microscope. Images were captured using the same exposure time for each comparative section. To examine the specificity of immunostaining, the primary antibody was replaced with normal rabbit IgG (1 μg/ml). Control slides were invariably negative under the same setting (data not shown). For all experiments, at least three sections from each eye were evaluated. To demonstrate the expression patterns of HMGB1 in retinal cells under oxidative stress *in vitro*, R28 cells (2×10^5 cells/500 μl medium per well) were seeded on four-well glass coverslips and challenged with or without hydrogen peroxide (1 mM) for 1 h. Slides were fixed in 4% paraformaldehyde for 1 h, permeabilized with Triton X-100, and then examined by the same methods as described above.

ELISAs

HMGB1 and MCP-1 were quantified in each human vitreous sample using commercial ELISAs; HMGB1 ELISA kit (Shino-Test Corporation) and Human CCL2/MCP-1 Immunoassay (R&D Systems, Minneapolis, MN), according to the manufacturers' protocols. The detection limits of these kits were 0.2 ng/ml for HMGB1 and 5.0 pg/ml for MCP-1. Concentrations below the limits were taken as zero in subsequent analyses. Each sample was run in duplicate and compared with a standard curve. All samples were assessed in a masked manner. The mean concentration was determined per sample. For *in vitro* study, HMGB1 levels in culture supernatants were measured by the same ELISA.

Migration Assay

Cell migration was assayed using a modified Boyden chamber assay as previously described.[26] In brief, 5×10^4 ARPE-19 cells resuspended in 200 μl control medium (1% FBS-DMEM/F12) were seeded onto the upper compartment of the BD Falcon® culture inserts (BD Bioscience, San Jose, CA) with an 8-μm diameter pore size membrane in a 24-well companion plate. The lower chamber was filled with control medium (negative control) and those containing 50, 100, or 200 ng/ml rHMGB1. Because MCP-1 was reported to display a potent chemotactic activity on RPE cells,[27] a control medium containing 10 ng/ml rMCP-1 was used as a positive control. After 8-h incubation, cells remaining on the upper surface of the filters were removed mechanically, and those that had migrated to the lower surface were fixed with methanol, stained with Diff-Quick (Dade-Behring, Deerfield, IL), and counted in five randomly selected high-power fields ($\times$ 100) per insert. Migration index (% of control) was calculated by dividing the number of migrating cells in the presence of chemoattractants by the cells that migrated in response to the negative control. To inhibit ERK-1/2 activity, the cells were pretreated with 1, 5, or 10 μM U0126, or vehicle (0.1% dimethyl sulfoxide) for 30 min, prior to the addition of rHMGB1. U0126 is an inhibitor of active and inactive MEK-1/2, the MAPK kinase that activates ERK-1/2. These concentrations of U0126 and dimethyl sulfoxide had no effect on ARPE-19 cell viability determined by MTT assay in our study (data not shown) and in a previous report.[28] Assays were performed in triplicate and repeated three times in independent experiments.

Immunoblotting

ARPE-19 cells (5×10^5) were subcultured on 6-cm tissue culture dishes. Then, the cells were serum starved overnight in DMEM/F12 and stimulated with 100 ng/ml rHMGB1 for the indicated times. Activation of ERK-1/2 was analyzed as described previously.[24] In brief, after treatment, whole cells were lysed with SDS sample buffer and an equal volume of protein extracts was loaded onto 12% SDS-polyacrylamide gels and then transferred onto a nitrocellulose membrane. The membrane was blocked by incubation with 5% non-fat dry milk plus 1% BSA in TBST (0.02% Tween-20 in Tris-buffered saline, pH 7.4) for 1 h at room temperature. The membrane was then incubated with the antibody against phospho-ERK-1/2 (diluted 1/1000) at 4°C overnight. The blots were subsequently probed with secondary anti-rabbit antibodies conjugated to horseradish peroxidase (diluted 1/3000 in TBST), and images were developed using the en-

hanced chemiluminescence system (GE Healthcare). The membrane was stripped and reprobed with an antibody against total ERK-1/2 (diluted 1/1000).

Statistical Analysis

The vitreous HMGB1 and MCP-1 concentrations in each group were compared using the Mann–Whitney *U*-test. The correlation between HMGB1 and MCP-1 in RD samples was analyzed using a simple linear regression analysis and Spearman's rank correlation coefficient. All *in vitro* data are presented as mean ± s.d. and the significance of differences between groups was determined by Student's *t*-test. *P*-value less than 0.05 was considered significant.

RESULTS

HMGB1 is Present in Cultured Retinal Cell and Released Extracellularly by Oxidative Stress-Induced Cell Death

We first evaluated the expression patterns and cellular distribution of HMGB1 in an R28 retinal cell line with or without oxidative stress, a known cause of neurodegeneration.[29] Excessive reactive oxygen species can lead to the destruction of cellular components and ultimately induce cell death through apoptosis or necrosis. To induce oxidative stress, we used a toxic dose (1 mM) of hydrogen peroxide, which was reported to stimulate monocytes/macrophages to release HMGB1 actively and passively.[30] As shown in Figure 1a, HMGB1 immunoreactivity was stably present in the nucleus of unstimulated R28 cells, and relatively weak staining was observed in the cytoplasm. By contrast, 1 h after exposure to 1 mM hydrogen peroxide, some cells seemed to present rather high levels of HMGB1 in their nucleus as well as their cytoplasm compared with those under an unstimulated condition. However, in the other cells, the nuclear HMGB1 was diminished or appeared to be released into the cytoplasm. These results indicate that the nuclear HMGB1 could be varied by death stress and be released into the cytoplasm according to the degree of stress. Hydrogen peroxide (1 mM) treatment for 24 h, in which about 90% of the cells lost their viability (Figure 1b), induced a massive release of HMGB1 from the cells to the cell supernatants (Figure 1c). Taken together, these findings suggested that HMGB1 could relocate from the nucleus to the cytoplasm for eventual release in dying retinal cells, and that the extracellular release of HMGB1 in the eye might be increased dependent on the extent of retinal cell death.

HMGB1 is Abundantly Expressed in Rat Retina and Released after RD

As the above findings indicated that HMGB1 was of relevance to retinal cell death, we investigated whether HMGB1 was maintained in the rat retina and how HMGB1 would vary after RD. As it was reported that HMGB1 in rat photoreceptors had a light-sensitive circadian rhythmic expression,[25] we performed all animal studies on a regular time schedule, and all eyes were set to be almost equally exposed to light. As shown in Figure 2, HMGB1 immunoreactivity was well represented in sections of the normal control rat retina and, as expected, colocalized with DAPI-positive nuclei (Figure 2a, d and g). HMGB1 staining in the normal rat retina was prominent in the nuclei of ganglion cell layer, inner nuclear layer, outer nuclear layer, and RPE, and was also apparent in the photoreceptor inner segments. In particular, HMGB1 was localized in photoreceptor at the nuclear periphery, and HMGB1 levels were higher in the inner nuclear layer than the outer nuclear layer as opposed to DAPI staining, which preferred to bind to heterochromatic DNA. This was consistent with the previous report[25] that HMGB1 was preferentially colocalized with euchromatin, which was often under active transcription and was stained less by DAPI. Interestingly, HMGB1 appeared to be robustly upregulated in both the photoreceptors and the other retinal cells at day 3 after RD inductions, and DAPI staining was inversely downregulated at the same time (Figure 2b, e and h). As previous reports demonstrated that dramatic alterations of retinal gene expression occurred after RD,[31] this high level of HMGB1 expression might be related to the active gene transcription. HMGB1 in the nucleus might be stress responsive and necessary for proper transcription after RD tissue damage. Afterwards, the nuclear HMGB1 expression in the photoreceptors seemed to subside at day 7, while still clearly remained in the inner segments (Figure 2c, f and i), gradually decreasing along with the thinning of the outer nuclear layer due to photoreceptor degeneration by day 14 (data not shown).

Although HMGB1 expression was increased in the photoreceptors of the detached retina at day 3, it was not homogeneous, but was rather heterogeneous. To clarify the relationship between the upregulation of HMGB1 and photoreceptor cell death, especially with DNA damage, the RD retina at day 3 was co-stained with TUNEL, which could detect apoptotic and potentially necrotic cell death by labeling the damaged DNA (Figure 3a–c). Previous studies indicated that HMGB1 could not be released from apoptotic cells[6] and the apoptotic photoreceptors were prominent in this RD model at day 3 after RD.[22] We also confirmed remarkable numbers of apoptotic photoreceptors in the detached retina at day 3 (Figure 3b), and found that the early faint TUNEL-positive nuclei had relatively low levels of HMGB1 and fragmented nuclei, which were brightly stained by TUNEL, had almost no apparent HMGB1 immunoreactivity (Figure 3c), suggesting that apoptotic dying cells might lose the expression of HMGB1 to maintain the proper gene transcription. It might be indispensable for the surviving photoreceptors to maintain and/or boost the nuclear HMGB1 in RD.

In the subretinal space of RD at day 7, HMGB1-positive and TUNEL-negative debris could be observed (Figure 3d, arrows), which might be released by necrotic photoreceptors and/or degradated inner segments, and spread diffusely into the vitreous cavity if a retinal break was present. It was also

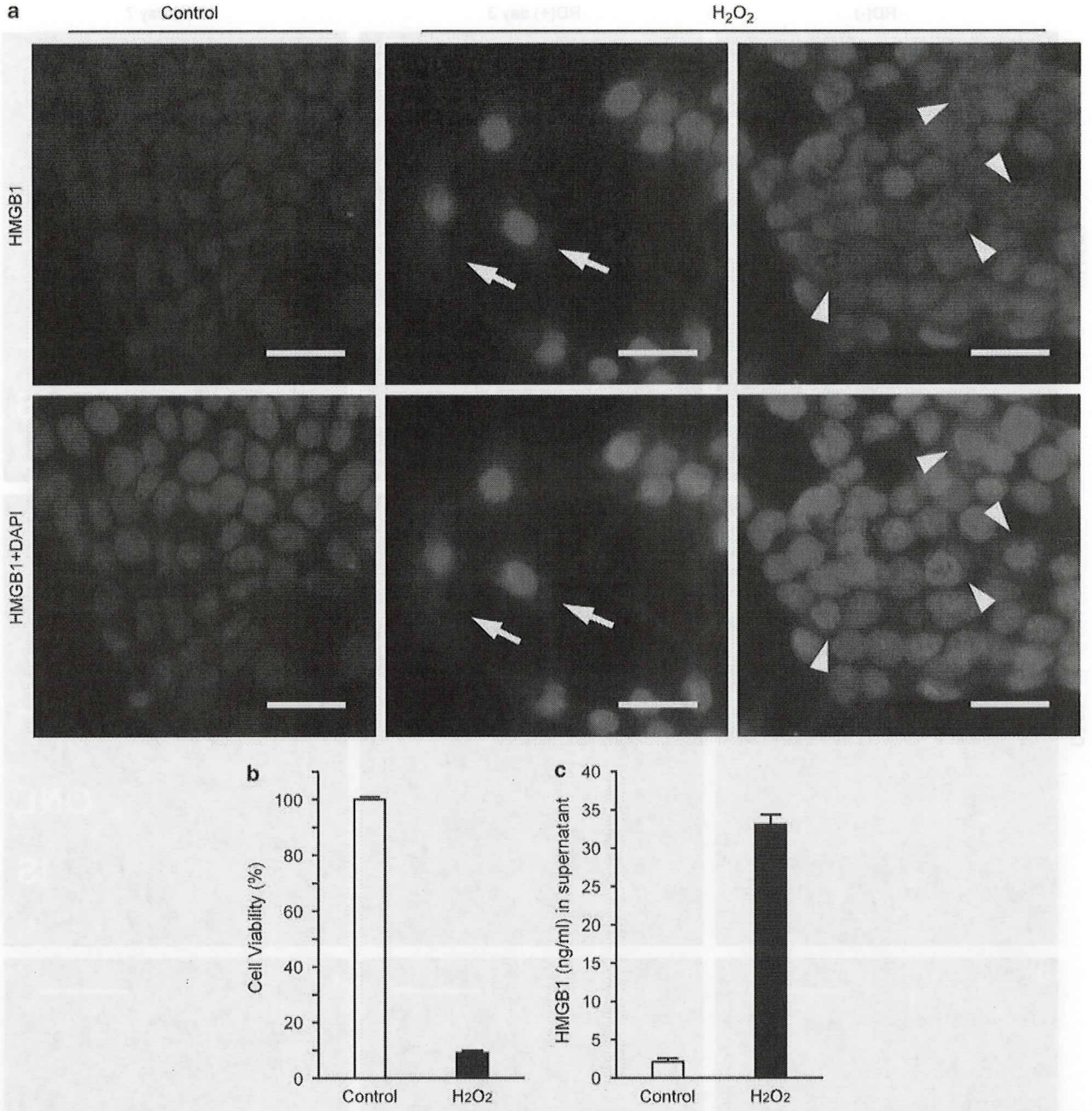

Figure 1 Release of HMGB1 from R28 retinal neuronal cells exposed to excessive oxidative stress. (**a**) Immunofluorescence was performed with anti-HMGB1 antibody (red) and DAPI (blue). HMGB1 is predominantly present in the nuclei of unstimulated R28 cells (left column). Some cells present robust upregulation of HMGB1 in the nuclei, as well as relocation into the cytoplasm (middle column; arrows) on 1 h exposure to a toxic dose of hydrogen peroxide (1 mM). In the other cells, the nuclear HMGB1 is found to be diminished or released into the cytoplasm (right column; arrowheads). Scale bars: 20 μm. (**b**) After 24 h exposure to 1 mM hydrogen peroxide, the cell viability analyzed by MTT assay is decreased to about 10% compared with the control. (**c**) Massive HMGB1 release into the culture supernatant was determined by ELISA after the same treatment as (**b**). The data represent the mean ± s.d. ($n = 3$). Similar results were obtained from three independent experiments.

Figure 2 Immunofluorescence analysis of HMGB1 in a rat model of RD. Representative photomicrographs of retinal sections labeled with anti-HMGB1 antibody (red; **a–c**) and DAPI (blue; **d–f**). Merged images (**g–i**) are also presented. The retinal sections were derived from the control eye (**a, d, g**), those at 3 days (day 3; **b, e, h**), or 7 days after RD (day 7; **c, f, i**). Arrows point to retinal pigment epithelium (**a, g**), and arrowheads indicate subretinal macrophages (**b, c, h, i**). Note that expression of HMGB1 is augmented especially in ONL at day 3 after RD, whereas the upregulation in ONL appears to be subside by day 7 ($n = 6$ for each time point). Scale bars: 50 μm. INL, inner nuclear layer; IS, inner segment; ONL, outer nuclear layer.

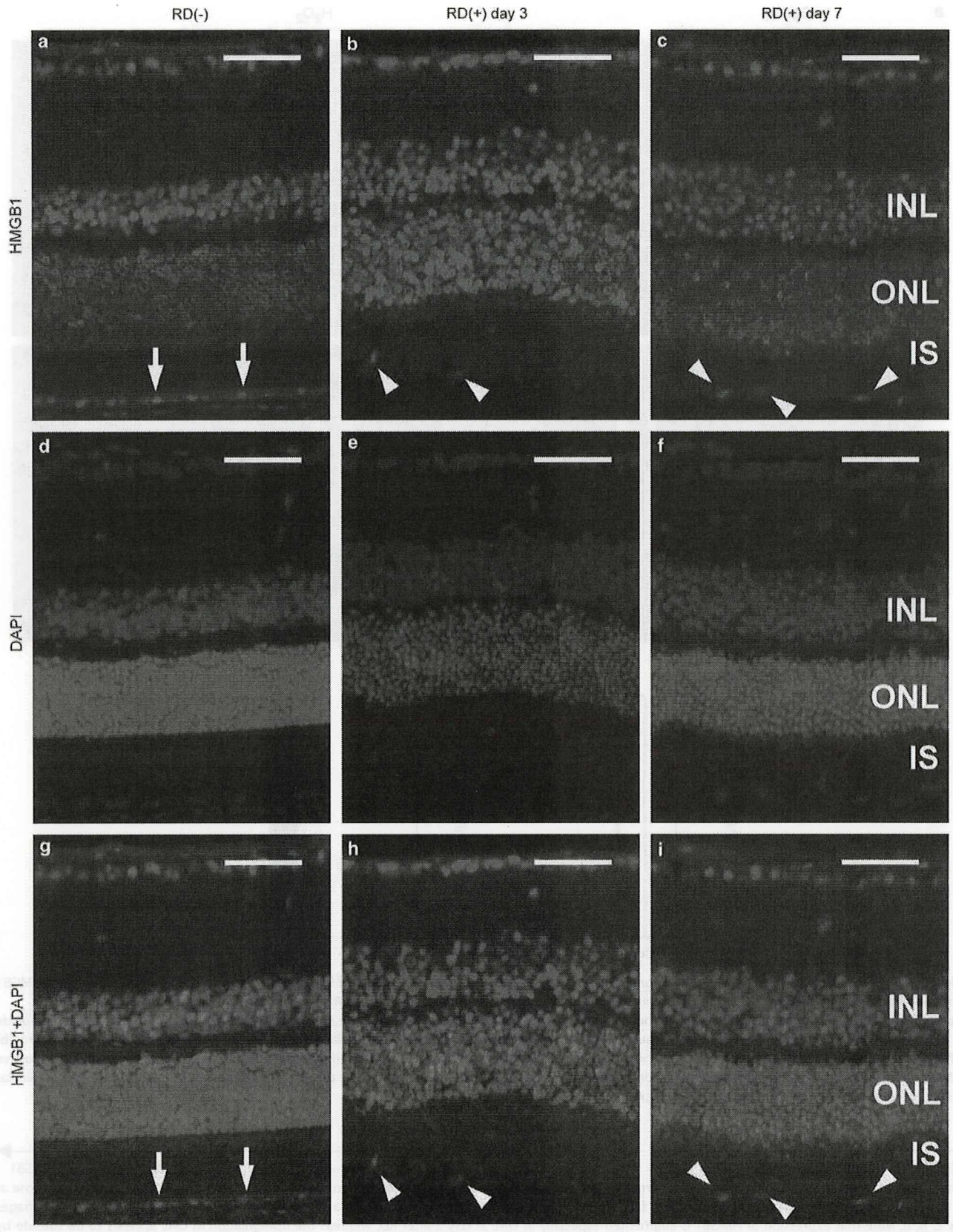
RD(-)
RD(+) day 3
RD(+) day 7
HMGB1
DAPI
HMGB1+DAPI
a
b
c
d
e
f
g
h
i
INL
ONL
IS

reported that macrophages migrated into the subretinal space of this RD model.[32] The migrating macrophages also had abundant HMGB1 expression (Figure 3d, arrowheads), and might have released HMGB1 actively in this space. In line with these data, a large amount of extracellular HMGB1 must be present at least in the subretinal space after RD.

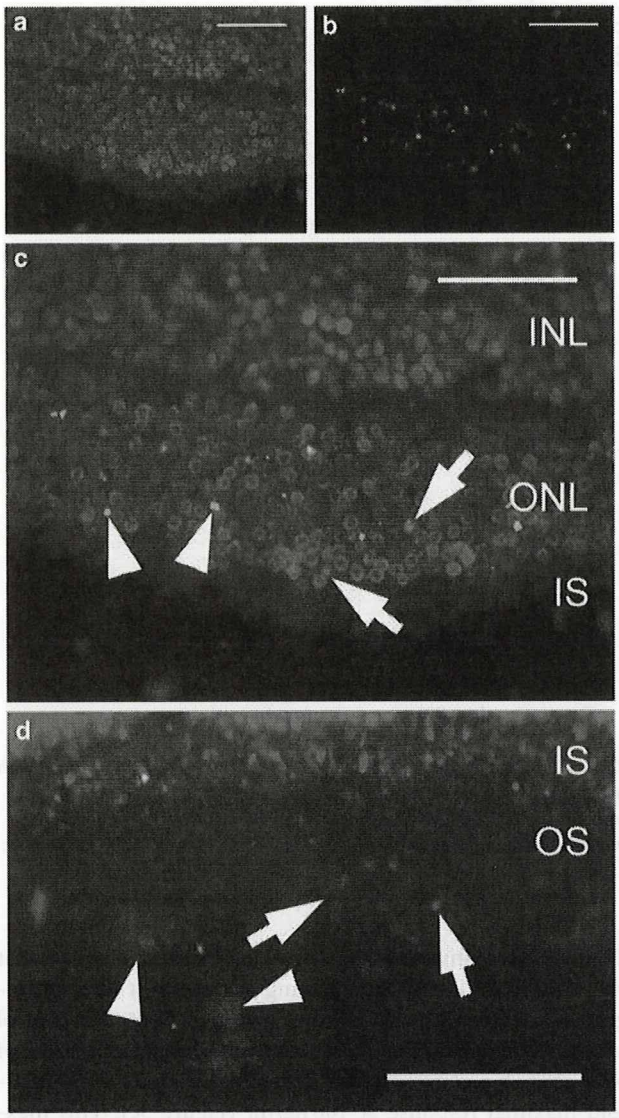

Figure 3 Expression of HMGB1 in DNA-damaged photoreceptors (**a–c**) and release of HMGB1 in the subretinal space (**d**). Representative photomicrographs of anti-HMGB1 antibody (red; **a**), TUNEL (green; **b**), and merged image (**c**) from rat retinal sections at 3 days after RD ($n=6$). The early faint TUNEL-positive nuclei (**c**; arrows) have relatively low levels of HMGB1 and the fragmented nuclei (**c**; arrowheads) have almost no apparent HMGB1 immunoreactivity. (**d**) Representative photomicrograph of a merged image of anti-HMGB1 (red), DAPI (blue), and TUNEL (green) obtained from rat retinal sections at 7 days after RD ($n=6$). HMGB1-positive and TUNEL-negative debris (**d**; arrows) and migrating macrophages with abundant HMGB1 expression (**d**; arrowheads) can be observed in the subretinal space. Scale bars: 50 μm. INL, inner nuclear layer; IS, inner segment; ONL, outer nuclear layer; OS, outer segment.

Vitreous HMGB1 and MCP-1 Levels in Patients with RD

The result obtained from the rat model of RD is the first evidence to our knowledge that HMGB1 is involved in RD-induced photoreceptor degeneration. Next, we tested whether extracellular HMGB1 could also be detected in human vitreous samples of RD. Samples were harvested from 35 eyes with RD, including rhegmatogenous RD, RD with macular hole, and atopic RD and 19 eyes with control diseases, including idiopathic epiretinal membrane and idiopathic macular hole (Table 1). The vitreous HMGB1 and MCP-1 levels were significantly higher in the eyes with RD than in those with control diseases (Figure 4). The median HMGB1 level was 1.4 ng/ml (range, 0–28.3) in the eyes with RD and 0.6 ng/ml (range, 0–1.3) in those with control diseases ($P<0.001$; Figure 4a). The median MCP-1 level was 1383.2 pg/ml (range, 39.8–5436.1) in the RD eyes and 404.4 pg/ml (range, 17.9–1168.9) in the control eyes ($P<0.0001$; Figure 4b). The vitreous concentration of HMGB1 was correlated significantly with that of MCP-1 in the 35 eyes with RD by a simple linear regression ($r=0.593$, $P<0.001$; Figure 4c) and by Spearman's rank correlation coefficient ($r=0.613$, $P<0.001$). On the other hand, there was no significant relationship between the vitreous concentrations of HMGB1 and MCP-1 in the 19 eyes of control patients (data not shown). Although there was no significant difference, the HMGB1 levels in the eyes with proliferative vitreoretinopathy (PVR), a condition of retinal fibrosis that follows severe long-standing RD, tended to be lower than those without PVR (Figure 4d). These findings showed that HMGB1 could be released not only in the subretinal space but also in the vitreous cavity after RD-induced photoreceptor degeneration, and that the HMGB1 release was coincident with vitreous MCP-1 expression.

Table 1 Characteristics of the patients

Characteristics	Retinal detachment ($n=35$)	Control diseases ($n=19$)
Age (years)	57.3 ± 16.3	68.2 ± 8.7
Female sex, no. (%)	19 (54)	10 (53)
Patients with PVR, no. (%)	6 (17)	—
Subgroups, no. (%)		
Rhegmatogenous retinal detachment	28 (80)	—
Retinal detachment with macular hole	5 (14)	—
Atopic retinal detachment	2 (6)	—
Idiopathic epiretinal membrane	—	7 (37)
Idiopathic macular hole	—	12 (63)

PVR, proliferative vitreoretinopathy.
Values are expressed as mean ± s.d. Dashes denote not applicable.

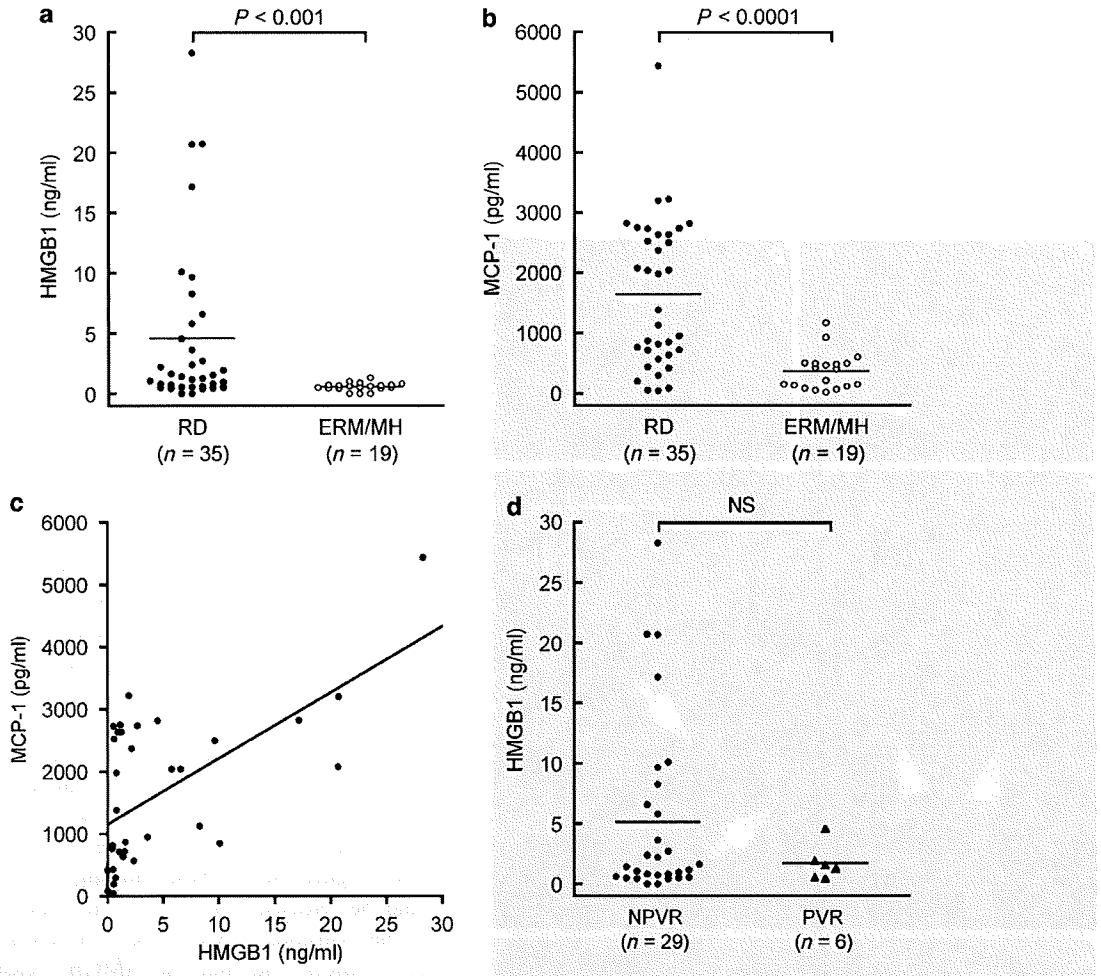

Figure 4 Vitreous levels of HMGB1 and MCP-1. The vitreous HMGB1 (**a**) and MCP-1 (**b**) levels are significantly higher in eyes with RD than in those with control diseases (idiopathic epiretinal membrane or idiopathic macular hole). Each bar indicates the average value. (**c**) Scatter plot for the correlation between vitreous levels of HMGB1 and MCP-1 in eyes with RD (simple linear regression, $r = 0.593$, $P < 0.001$; Spearman's rank correlation coefficient, $r = 0.613$, $P < 0.001$). (**d**) The HMGB1 levels in the eyes with PVR tend to be lower than those without PVR. ERM/MH, epiretinal membrane/macular hole; NPVR, no PVR; PVR, proliferative vitreoretinopathy.

RPE Cells Respond Chemotactically to Extracellular HMGB1 through an ERK-Dependent Mechanism

Previous reports have shown that extracellular HMGB1 is a chemoattractant for a variety of cell types.[21,33,34] We investigated whether HMGB1 is also a chemoattractant for RPE cells. Extracellular HMGB1 has been reported to engage multiple receptors, including the receptor for advanced glycation end products (RAGE) and Toll-like receptors 2 and 4.[2,4] In particular, RAGE has been thought to be a crucial receptor for HMGB1-induced cell migration through ERK activation.[33] The expression of RAGE at the RNA and protein level was identified in human RPE[35] and ARPE-19 cells[36,37] in previous studies. It was also shown that the expression of RAGE and HMGB1 was colocalized in the proliferative membrane from an eye with proliferative retinal disease.[38] We, therefore, performed a migration assay using modified Boyden chambers with various concentrations of rHMGB1. The representative photographs in Figure 5 show that rHMGB1 was capable of inducing a significant level of migration (Figure 5b) above that obtained with the control medium (Figure 5a). HMGB1 stimulated the migration of RPE cells in a concentration-dependent manner with a 2.7-fold maximal response at 100 ng/ml (Figure 5c). This maximal response to rHMGB1 was slightly stronger than that induced by rMCP-1 (10 ng/ml). Next, we investigated whether HMGB1 induced phosphorylation of ERK-1/2 in ARPE-19 cells; we stimulated cells with 100 ng/ml rHMGB1 for various time periods and used western blotting with an anti-phospho-ERK-1/2 antibody on whole-cell lysates (Figure 6a). Little phosphorylation of ERK-1/2 could be observed in unstimulated ARPE-19 (at 0 min), but a prominent increase was detected after 5 min of stimulation with rHMGB1. Figure 6a shows that phosphorylation of ERK-1/2 was augmented from 5 to 60 min after rHMGB1 stimulation in comparison

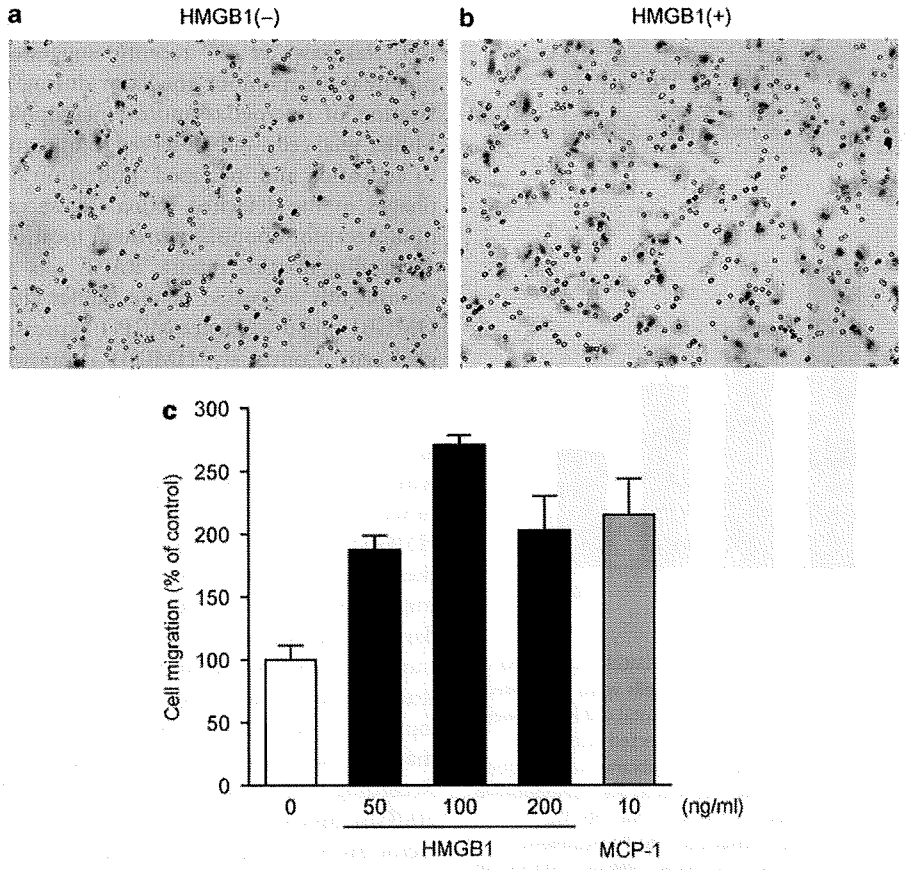

Figure 5 RPE cells migrate in response to HMGB1. Representative photographs of ARPE-19 cells stained with Diff-Quick after migration toward control medium (**a**) or 100 ng/ml HMGB1 (**b**). Original magnification: ×100. (**c**) HMGB1 stimulated ARPE-19 cell migration in a concentration-dependent manner with a 2.7-fold maximal response at 100 ng/ml. The data represent the mean ± s.d. ($n = 3$). All treatments increase the migratory response relative to the control ($P < 0.01$ in Student's *t*-test). Similar results were obtained from three independent experiments.

with unstimulated ARPE-19 (time 0). To demonstrate that the ERK signaling induced by HMGB1 was in fact linked to the migration of RPE cells, we next inhibited ERK-1/2 and assessed cell migration to HMGB1. Pretreatment of ARPE-19 with U0126 abrogated the migration toward rHMGB1 (Figure 6b). Thus, the ERK pathway appears to play an essential role in HMGB1-induced RPE cell migration.

DISCUSSION

Our findings suggest a possible role of HMGB1 in RD, as an essential nuclear protein and a principal danger signal for photoreceptor degeneration. Using an *in vitro* assay of retinal cell death induced by excessive oxidative stress, we found that HMGB1 was augmented in the nucleus by the stress and released into the extracellular space during cell death. On the basis of immunohistochemical analyses of a rat model of RD-induced photoreceptor degeneration, augmentation of HMGB1 in the nucleus is also observed *in vivo* and appears to be crucial for the proper transcription of photoreceptors after RD. Moreover, double labeling with TUNEL reveals defects of upregulation of the nuclear HMGB1 in the DNA-damaged photoreceptors, which are presumably programmed dying photoreceptors. Therefore, we propose that the nuclear HMGB1 in the retinal cells might be critical for retinal cell survival under death stresses both in the *in vivo* RD and *in vitro* retinal cell death. These results for ocular HMGB1 are compatible with previous reports that HMGB1 is a vital nuclear protein and has a protective role in the nucleus.[2,4]

In a previous animal study, Erickson *et al*[17] reported that a loss of photoreceptors in a cat model of RD occurred due to necrosis. During studies on RD, photoreceptor degeneration after RD had been thought to be mainly caused by apoptosis.[15,16] Hisatomi *et al*[32] demonstrated the presence of apoptotic debris in the subretinal space of rat RD. In the present study, considering our immunohistochemistry results from the same rat model of RD, so-called necrotic debris, which is HMGB1 positive and TUNEL negative, was found to be present. On the basis of the previous finding of the preferential release of HMGB1 from necrotic cells,[6] this suggests that necrosis might still be a fundamental type of photoreceptor cell death after RD.

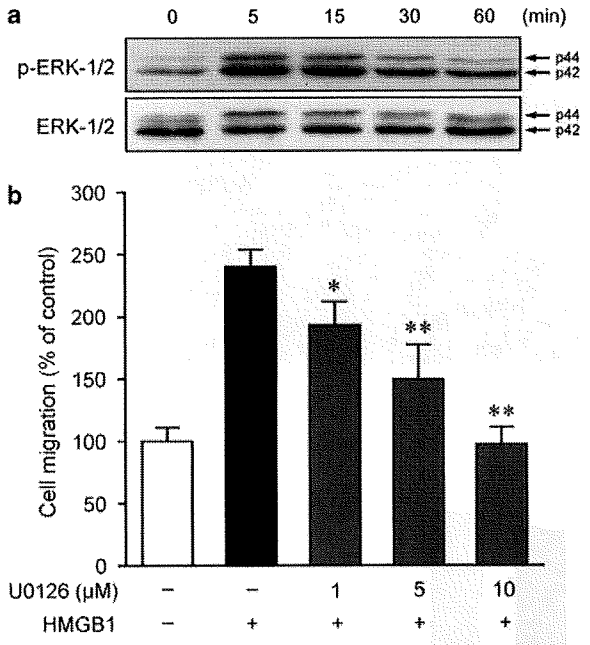

Figure 6 The phosphorylation of ERK is induced by HMGB1 and linked to HMGB1-induced migration of RPE cells. (**a**) ARPE-19 cells were stimulated with HMGB1 (100 ng/ml) for 5, 15, 30, or 60 min, and total cell lysates were analyzed by western blot. ERK-1/2 activation was detected with anti-phospho-ERK-1/2 antibody (p-ERK-1/2). Stripped membrane was reprobed with the antibody against total ERK-1/2 (ERK-1/2). Results are representative of three independent experiments. HMGB1 augments the ERK-1/2 phosphorylation from 5 to 60 min after stimulation. (**b**) Pretreatment of ARPE-19 with U0126 inhibits the cell migration toward HMGB1 (100 ng/ml) in a dose-dependent manner. The data represent the mean ± s.d. ($n = 3$). Similar results were obtained from three independent experiments. $^*P<0.05$, $^{**}P<0.01$, compared with vehicle-treated control.

Furthermore, exploring human vitreous samples by ELISA, we found that both HMGB1 and MCP-1 are increased significantly in eyes with RD. Although MCP-1 is a well-known mediator for RD,[39] to our knowledge, this is the first report indicating that extracellular HMGB1 might also be of relevance to human RD. HMGB1 concentration tended to be high in the eye without PVR, but not so with PVR. One possible explanation for this tendency is that HMGB1 might be sequestered and/or masked in PVR, the advanced stage of RD. HMGB1 binds tightly to heparin and proteoglycans with heparan sulfate,[5] and it is also reported that such proteoglycans are abundantly present as the ocular extracellular matrix, even in RD.[40] Hence, these molecules might affect the HMGB1 concentration in the vitreous humor. Nevertheless, this possibility does not negate the presence of HMGB1. Considering the results obtained with the rat RD model, extracellular HMGB1 could be present at much higher levels, at least in the subretinal fluid of RD, and it might serve as a persistent signal adhering to the local damaged retina and/or surrounding matrix as previously described.[5]

It is also of importance that HMGB1 is significantly correlated with MCP-1 in RD vitreous. The secretion of MCP-1 might parallel the extent of photoreceptor degeneration of RD. Nakazawa *et al*[20] recently suggested that MCP-1 is a potential proapoptotic mediator during RD through the activation of microglias and/or macrophages. In their study, Müller-glial cells were observed to upregulate MCP-1, leading to activation and increased infiltration of microglias/macrophages in the detached retina. These cells induced further photoreceptor apoptosis through local oxidative stress. Corresponding to this report, RAGE was also reported to be prominently expressed in the Müller-glial cells.[41] Therefore, HMGB1 might influence MCP-1 expression through Müller-glial cells. Conversely, HMGB1 is known to be released by activated monocytes/macrophages.[7] MCP-1 is a potent stimulator and chemoattractant for monocytes/macrophages,[42] and these cells were observed in the subretinal space of RD with abundant HMGB1 expression. This would also be another possible explanation for the parallel increases of HMGB1 and MCP-1. Nevertheless, the positive correlation of these molecules indicates that cell death-related mediators might be highly orchestrated in ocular degenerative tissue damage. Several studies suggest that extracellular HMGB1 can aggravate tissue damage in neuronal tissues.[10,43] In these studies, extracellular HMGB1 plays a key role in the development of neuronal injury through the induction of inflammation, microglial activation, and neuronal excitotoxicity. According to these recent reports, the presence of extracellular HMGB1 concomitantly with MCP-1 is a possible deteriorating factor for RD, in spite of its essential role in the nucleus.

PVR is one of the most threatening complications of RD. It is thought to be a reactive process to retinal injury, in other words, it is one of the wound-healing responses in the eye. RPE cells are known to be detectable in the fibrotic proliferative membranes of PVR, and play an important role in the pathogenesis of PVR.[44] Thus, the effects of a molecule on PVR formation could be traced to RPE migration, at least in part. Here, we demonstrate that extracellular HMGB1 promotes RPE cell migration by chemotaxis *in vitro*. This result is consistent with previous reports of HMGB1-induced cell migration in various cell types, such as smooth muscle cells,[21,33] fibroblasts,[45] and chondrocytes.[34] We also found that HMGB1 activated phosphorylation of ERK-1/2 in RPE cells and the migration induced by HMGB1 was dependent on ERK phosphorylation. The phosphorylation of ERK is associated with cell proliferation and cell migration through effects on cell–matrix contacts.[46] It was also reported to be found in Müller-glial cells after RD.[47] Taken together, our results suggest that extracellular HMGB1 from dying ocular cells might affect retinal cells through ERK phosphorylation and potentially serve to promote the formation of PVR, which is wound healing, but has a pathological meaning in the eye. Several new strategies for prevention of ocular fibrosis, especially targeting specific signaling pathways, have been proven to be beneficial in animal models.[48–50] We propose that the identification and further characterization of danger signals, including HMGB1, would provide a novel

perspective for better understanding the molecular pathogenesis of PVR before applying these promising therapeutic manipulations to human subjects.

It has been suggested that post-transcriptional modifications of HMGB1, such as acetylation, methylation, and phosphorylation, might influence its activity.[51] Some recent reports also demonstrate that the proinflammatory activity of HMGB1 is due to combined action with other molecules.[52] The present data are mostly limited to the presence of HMGB1 rather than its biological activity, and we do not address what modifications or molecules are involved in intraocular HMGB1. However, we identify for the first time that HMGB1 is evident in a typical retinal injury of human RD, in which nuclear HMGB1 is a crucial nuclear protein and extracellular HMGB1 is a danger signal that might be required for the ocular wound-healing response. Our findings might have relevance for the underlying mechanisms of degenerative neuronal diseases. Further detailed studies will be needed to obtain more accurate knowledge and therapeutic value of HMGB1 in human diseases.

ACKNOWLEDGEMENTS

We thank Dr GM Siegel, The State University of New York, for providing R28 cells; Drs Takashi Ito, Yoko Oyama, Toshiaki Shimizu, Kazunori Takenouchi, Kiyoshi Kikuchi, Masahiro Iwata, Yuko Nawa, Yoko Morimoto, Naoki Miura, and Noboru Taniguchi for their helpful advice and technical support; Miss Nobue Uto, Tomoka Nagasato, Hisayo Sameshima, and Maiko Yamaguchi for their assistance with the experiments. This research was supported in part by a grant from the Research Committee on Chorioretinal Degeneration and Optic Atrophy, Ministry of Health, Labor, and Welfare and by a grant-in-aid for Scientific Research from the Ministry of Education, Science, and Culture of the Japanese Government.

1. Bianchi ME. DAMPs, PAMPs and alarmins: all we need to know about danger. J Leukoc Biol 2007;81:1–5.
2. Ulloa L, Messmer D. High-mobility group box 1 (HMGB1) protein: friend and foe. Cytokine Growth Factor Rev 2006;17:189–201.
3. Martin P. Wound healing—aiming for perfect skin regeneration. Science 1997;276:75–81.
4. Lotze MT, Tracey KJ. High-mobility group box 1 protein (HMGB1): nuclear weapon in the immune arsenal. Nat Rev Immunol 2005;5:331–342.
5. Huttunen HJ, Rauvala H. Amphoterin as an extracellular regulator of cell motility: from discovery to disease. J Intern Med 2004;255:351–366.
6. Scaffidi P, Misteli T, Bianchi ME. Release of chromatin protein HMGB1 by necrotic cells triggers inflammation. Nature 2002;418:191–195.
7. Wang H, Bloom O, Zhang M, *et al.* HMG-1 as a late mediator of endotoxin lethality in mice. Science 1999;285:248–251.
8. Passalacqua M, Patrone M, Picotti GB, *et al.* Stimulated astrocytes release high-mobility group 1 protein, an inducer of LAN-5 neuroblastoma cell differentiation. Neuroscience 1998;82:1021–1028.
9. Ito T, Kawahara K, Nakamura T, *et al.* High-mobility group box 1 protein promotes development of microvascular thrombosis in rats. J Thromb Haemost 2007;5:109–116.
10. Kim JB, Sig Choi J, Yu YM, *et al.* HMGB1, a novel cytokine-like mediator linking acute neuronal death and delayed neuroinflammation in the postischemic brain. J Neurosci 2006;26:6413–6421.
11. Campana L, Bosurgi L, Rovere-Querini P. HMGB1: a two-headed signal regulating tumor progression and immunity. Curr Opin Immunol 2008;20:518–523.
12. Inoue K, Kawahara K, Biswas KK, *et al.* HMGB1 expression by activated vascular smooth muscle cells in advanced human atherosclerosis plaques. Cardiovasc Pathol 2007;16:136–143.
13. Taniguchi N, Kawahara K, Yone K, *et al.* High mobility group box chromosomal protein 1 plays a role in the pathogenesis of rheumatoid arthritis as a novel cytokine. Arthritis Rheum 2003;48:971–981.
14. Morimoto Y, Kawahara KI, Tancharoen S, *et al.* Tumor necrosis factor-alpha stimulates gingival epithelial cells to release high mobility-group box 1. J Periodontal Res 2008;43:76–83.
15. Cook B, Lewis GP, Fisher SK, *et al.* Apoptotic photoreceptor degeneration in experimental retinal detachment. Invest Ophthalmol Vis Sci 1995;36:990–996.
16. Arroyo JG, Yang L, Bula D, *et al.* Photoreceptor apoptosis in human retinal detachment. Am J Ophthalmol 2005;139:605–610.
17. Erickson PA, Fisher SK, Anderson DH, *et al.* Retinal detachment in the cat: the outer nuclear and outer plexiform layers. Invest Ophthalmol Vis Sci 1983;24:927–942.
18. Vazquez-Chona F, Song BK, Geisert Jr EE. Temporal changes in gene expression after injury in the rat retina. Invest Ophthalmol Vis Sci 2004;45:2737–2746.
19. Arimura N, Ki IY, Hashiguchi T, *et al.* High-mobility group box 1 protein in endophthalmitis. Graefes Arch Clin Exp Ophthalmol 2008;246:1053–1058.
20. Nakazawa T, Hisatomi T, Nakazawa C, *et al.* Monocyte chemoattractant protein 1 mediates retinal detachment-induced photoreceptor apoptosis. Proc Natl Acad Sci USA 2007;104:2425–2430.
21. Porto A, Palumbo R, Pieroni M, *et al.* Smooth muscle cells in human atherosclerotic plaques secrete and proliferate in response to high mobility group box 1 protein. FASEB J 2006;20:2565–2566.
22. Hisatomi T, Sakamoto T, Murata T, *et al.* Relocalization of apoptosis-inducing factor in photoreceptor apoptosis induced by retinal detachment *in vivo*. Am J Pathol 2001;158:1271–1278.
23. Neekhra A, Luthra S, Chwa M, *et al.* Caspase-8, -12, and -3 activation by 7-ketocholesterol in retinal neurosensory cells. Invest Ophthalmol Vis Sci 2007;48:1362–1367.
24. Biswas KK, Sarker KP, Abeyama K, *et al.* Membrane cholesterol but not putative receptors mediates anandamide-induced hepatocyte apoptosis. Hepatology 2003;38:1167–1177.
25. Hoppe G, Rayborn ME, Sears JE. Diurnal rhythm of the chromatin protein Hmgb1 in rat photoreceptors is under circadian regulation. J Comp Neurol 2007;501:219–230.
26. Hinton DR, He S, Graf K, *et al.* Mitogen-activated protein kinase activation mediates PDGF-directed migration of RPE cells. Exp Cell Res 1998;239:11–15.
27. Han QH, Hui YN, Du HJ, *et al.* Migration of retinal pigment epithelial cells *in vitro* modulated by monocyte chemotactic protein-1: enhancement and inhibition. Graefes Arch Clin Exp Ophthalmol 2001;239:531–538.
28. Glotin AL, Calipel A, Brossas JY, *et al.* Sustained versus transient ERK1/2 signaling underlies the anti- and proapoptotic effects of oxidative stress in human RPE cells. Invest Ophthalmol Vis Sci 2006;47:4614–4623.
29. Klein JA, Ackerman SL. Oxidative stress, cell cycle, and neurodegeneration. J Clin Invest 2003;111:785–793.
30. Tang D, Shi Y, Kang R, *et al.* Hydrogen peroxide stimulates macrophages and monocytes to actively release HMGB1. J Leukoc Biol 2007;81:741–747.
31. Hollborn M, Francke M, Iandiev I, *et al.* Early activation of inflammation- and immune response-related genes after experimental detachment of the porcine retina. Invest Ophthalmol Vis Sci 2008;49:1262–1273.
32. Hisatomi T, Sakamoto T, Sonoda KH, *et al.* Clearance of apoptotic photoreceptors: elimination of apoptotic debris into the subretinal space and macrophage-mediated phagocytosis via phosphatidylserine receptor and integrin alphavbeta3. Am J Pathol 2003;162:1869–1879.
33. Degryse B, Bonaldi T, Scaffidi P, *et al.* The high-mobility group (HMG) boxes of the nuclear protein HMG1 induce chemotaxis and cytoskeleton reorganization in rat smooth muscle cells. J Cell Biol 2001;152:1197–1206.
34. Taniguchi N, Yoshida K, Ito T, *et al.* Stage-specific secretion of HMGB1 in cartilage regulates endochondral ossification. Mol Cell Biol 2007;27:5650–5663.
35. Yamada Y, Ishibashi K, Ishibashi K, *et al.* The expression of advanced glycation endproduct receptors in rpe cells associated with basal deposits in human maculas. Exp Eye Res 2006;82:840–848.

36. Howes KA, Liu Y, Dunaief JL, *et al.* Receptor for advanced glycation end products and age-related macular degeneration. Invest Ophthalmol Vis Sci 2004;45:3713–3720.
37. Ma W, Lee SE, Guo J, *et al.* RAGE ligand upregulation of VEGF secretion in ARPE-19 cells. Invest Ophthalmol Vis Sci 2007;48: 1355–1361.
38. Pachydaki SI, Tari SR, Lee SE, *et al.* Upregulation of RAGE and its ligands in proliferative retinal disease. Exp Eye Res 2006;82: 807–815.
39. Elner SG, Elner VM, Jaffe GJ, *et al.* Cytokines in proliferative diabetic retinopathy and proliferative vitreoretinopathy. Curr Eye Res 1995;14:1045–1053.
40. Wang JB, Tian CW, Guo CM, *et al.* Increased levels of soluble syndecan-1 in the subretinal fluid and the vitreous of eyes with rhegmatogenous retinal detachment. Curr Eye Res 2008;33:101–107.
41. Barile GR, Pachydaki SI, Tari SR, *et al.* The RAGE axis in early diabetic retinopathy. Invest Ophthalmol Vis Sci 2005;46: 2916–2924.
42. Matsushima K, Larsen CG, DuBois GC, *et al.* Purification and characterization of a novel monocyte chemotactic and activating factor produced by a human myelomonocytic cell line. J Exp Med 1989;169:1485–1490.
43. Pedrazzi M, Raiteri L, Bonanno G, *et al.* Stimulation of excitatory amino acid release from adult mouse brain glia subcellular particles by high mobility group box 1 protein. J Neurochem 2006;99:827–838.
44. Pastor JC, de la Rua ER, Martin F. Proliferative vitreoretinopathy: risk factors and pathobiology. Prog Retin Eye Res 2002;21:127–144.
45. Straino S, Di Carlo A, Mangoni A, *et al.* High-mobility group box 1 protein in human and murine skin: involvement in wound healing. J Invest Dermatol 2008;128:1545–1553.
46. Lawrence MC, Jivan A, Shao C, *et al.* The roles of MAPKs in disease. Cell Res 2008;18:436–442.
47. Nakazawa T, Takeda M, Lewis GP, *et al.* Attenuated glial reactions and photoreceptor degeneration after retinal detachment in mice deficient in glial fibrillary acidic protein and vimentin. Invest Ophthalmol Vis Sci 2007;48:2760–2768.
48. Saika S. TGFbeta pathobiology in the eye. Lab Invest 2006;86 :106–115.
49. Saika S, Yamanaka O, Nishikawa-Ishida I, *et al.* Effect of Smad7 gene overexpression on transforming growth factor beta-induced retinal pigment fibrosis in a proliferative vitreoretinopathy mouse model. Arch Ophthalmol 2007;125:647–654.
50. Saika S, Yamanaka O, Sumioka T, *et al.* Fibrotic disorders in the eye: targets of gene therapy. Prog Retin Eye Res 2008;27:177–196.
51. Bianchi ME, Manfredi AA. High-mobility group box 1 (HMGB1) protein at the crossroads between innate and adaptive immunity. Immunol Rev 2007;220:35–46.
52. Sha Y, Zmijewski J, Xu Z, *et al.* HMGB1 develops enhanced proinflammatory activity by binding to cytokines. J Immunol 2008;180:2531–2537.

Posturing Time after Macular Hole Surgery Modified by Optical Coherence Tomography Images: A Pilot Study

KYOKO MASUYAMA, KEITA YAMAKIRI, NOBORU ARIMURA, YASUSHI SONODA, NORIHITO DOI, AND TAIJI SAKAMOTO

• PURPOSE: To see the early postoperative stage of macular hole (MH) surgery and to distinguish eyes needing prolonged posturing from those that do not use Fourier-domain optical coherence tomography (FD-OCT).

• DESIGN: Interventional case series.

• METHODS: Sixteen eyes of 15 patients with MH underwent the protocol at Kagoshima University Hospital. After the pars plana vitrectomy with 16% SF_6 gas tamponade followed by posturing, the eyes were examined by FD OCT from 3 hours to the day after surgery. After MH closure was confirmed, posturing was stopped. Follow-up was performed for 4 months or longer. The main outcome measures included time and OCT finding of MH closure after surgery.

• RESULTS: On the day after surgery, the macula could be examined by FD-OCT in 13 of 16 eyes; 10 eyes had a closed MH and 3 had an unclosed MH. At day 2, 2 of the 3 eyes with unclosed MHs on day 1 demonstrated a closed MH. Posturing continued for 8 days in 4 eyes whose MH closure was not confirmed. The MH was closed in all eyes within 1 month. FD-OCT showed bridge formation of the neural retina in 9 eyes and simple closure in 3 eyes within 7 days. At 1 month, 12 eyes showed simple closure and 4 eyes showed bridge formation. Among 9 eyes with bridge formation within 7 days, 6 eyes had changed to simple closure at 1 month.

• CONCLUSIONS: FD-OCT enabled confirmation of MH closure the day after surgery even in gas-filled eyes. This imaging method may be a good indicator to determine when to stop posturing for each patient. (Am J Ophthalmol 2009;147:481–488. © 2009 by Elsevier Inc. All rights reserved.)

SINCE KELLY AND WENDEL'S REPORT, IDIOPATHIC macular hole (MH) has become a treatable disease, and the recent anatomic success rate of MH closure is more than 90%.[1–6] Despite such a high success rate, there is still much room for improvement with this treatment. For example, the requirement for prolonged face-down posturing is a major burden on patients and physicians.[7,8]

Since Tornambe and associates' challenge, there has been a trend to shorten the period of posturing.[9–18] Some authors report that 1 day of posturing is equivalent to 1 week of posturing,[10] and other reports show that air tamponade followed by shorter posturing is equally effective for MH closure as is a long period of gas tamponade with prolonged posturing.[7,17] However, there are still concerns that shorter posturing may cause MH surgery to fail in some eyes, whereas prolonged posturing may cause most patients needless suffering. Therefore, a tailor-made postoperative program would be much more desirable rather than the uniform program largely followed now.

To devise a personally based approach, it is essential to monitor the very early stage of the MH closing process after surgery, especially during the gas-filled period; however, only a few studies have documented this process at the very early phase of the postoperative period. Takahashi and Kishi reported 2 closure patterns, bridge formation or simple closure, in the early phase after surgery using optical coherence tomography (OCT).[19] However, their observations were made 1 month after surgery, which did not reflect the very early phase of MH closure, and the information is not necessarily helpful for determining the duration of posturing. More recently, Hasler and Prünte showed OCT findings for 2 eyes on the first postoperative day through vitreous humor, but not gas-filling.[17]

Optical coherence tomography has made a great contribution to determining retinal pathologic features, including MH.[20–26] Nonetheless, the very early phase of MH closure after surgery cannot be observed in detail even with conventional (time-domain [TD]) OCT. One of the reasons is that clear imaging is hampered by a strong light reflex from the posterior surface in a gas-filled eye. Another reason is that TD-OCT cannot identify the macular area accurately in a gas-filled eye. Although no hole was found in the section of the possible macular area, this does not always mean the MH is closed, because the exact macula is not identifiable by TD-OCT. In contrast, Fourier-domain OCT (FD-OCT) has a function to scan a broad area within a short period, and serial scanning of a broad area allows more accurate identification and examination of the macula.[23]

In this study, the very early phase of the MH closure process was investigated using FD-OCT in eyes with full

Accepted for publication Sep 24, 2008.

Department of Ophthalmology, Kagoshima University Graduate School of Medical and Dental Sciences, Kagoshima, Japan.

Inquiries to Taiji Sakamoto, Department of Ophthalmology, Kagoshima University Graduate School of Medical and Dental Sciences, 8-35-1 Sakuragaoka, Kagoshima 890-8520, Japan; e-mail: tsakamot@m3.kufm.kagoshima-u.ac.jp

0002-9394/09/$36.00
doi:10.1016/j.ajo.2008.09.028

gas. This information would be important not only for a better understanding of the MH pathologic features, but also for reducing the burden on the patient with little risk through a tailor-made approach.

METHODS

ALL CONSECUTIVE PATIENTS WITH IDIOPATHIC MH WHO agreed to participate in this study from March 1, 2007 through February 29, 2008 were enrolled and a prospective study was performed. Data collected included patient age and gender, MH stage (Gass classification) and latency (judged by clinical history), cataract grade of mild (nuclear sclerosis 1+) or moderate to advanced (nuclear sclerosis 2+ or 3+), and Snellen best-corrected visual acuity (BCVA) before and after surgery. Postoperative adverse events such as infectious endophthalmitis, intraocular pressure rise, retinal detachment (RD), vitreous hemorrhage, choroidal detachment, and corneal pathologic features were noted. All surgeries were performed using local or general anesthesia (depending on patient general condition, preference, or both), and a standardized surgical procedure was used. All patients with a phakic eye received phacoemulsification cataract surgery with implantation of an intraocular lens (IOL). A 20-gauge standard pars plana vitrectomy (PPV) was performed, and the internal limiting membrane (ILM) was peeled with the help of triamcinolone (Kenacort-A; Bristol Pharmaceuticals KK, Tokyo, Japan), as in our previously described method.[27,28] After removing residual triamcinolone, the eye was flushed with 16% SF_6 gas and a maximum fill was attempted. All eyes were left firm after surgery with no documented leakage. The patients were postured face down as immediately as possible after surgery. If the patient agreed, the first OCT examination was performed 3 hours after surgery. Otherwise, the first OCT examination was performed every day from the day after surgery. When MH closure was found by OCT, the patients were asked to stop face-down posturing. This meant that the patients could assume any posturing, including during meals and for personal hygiene, although they were advised not to lie flat on their backs at night for 1 week to avoid IOL dislocation. The patients were followed up for 4 months or longer.

• **OPTICAL COHERENCE TOMOGRAPHY EXAMINATION AND DETERMINATION OF THE MACULA:** The posterior retina covering possible macular area was scanned with FD-OCT (Topcon, Tokyo, Japan) using a raster scan program. Using this system, 512 × 170 scans (horizontal × vertical) were possible within the 6 × 6-mm^2 area.[23] Thus, it is unlikely that an unclosed MH was overlooked by this method. MH closure by OCT was defined as no interruption of the internal line of the inner retina in any macular area. If MH closure was confirmed by this method, face-down posturing was discontinued regardless of residual gas in the vitreous cavity.

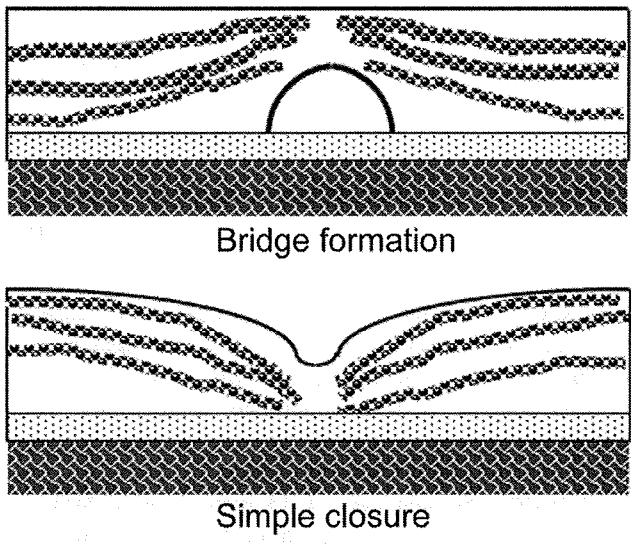

FIGURE 1. Diagrams illustrating optical coherence tomography (OCT) findings after macular hole (MH) surgery. (Top) Bridge formation type. (Bottom) Simple closure type.

Previously, OCT findings of MH at 1 month after surgery were classified as bridging formation or simple closure patterns.[19] Thus, the OCT findings after surgery that are presented herein were classified according to their criteria. Bridge formation type was defined as eyes that showed tissue that was continuous with the inner retina over the retinal pigment epithelium (RPE) that mimicked foveal RD (Figure 1), and simple closure type was defined as eyes that showed a normal foveal configuration from the initial examination.

RESULTS

THE STUDY INCLUDED 16 EYES OF 15 PATIENTS (7 EYES OF 6 females and 9 eyes of 9 male). Age ranged from 54 to 78 years. Preoperative BCVA ranged from 20/400 to 20/30 (mean, 20/200). The possible latency period before surgery ranged from 0 to 9 months. All eyes were phakic. Four eyes had a stage 2 MH (25%), 10 eyes had a stage 3 MH (62.5%), and 2 eyes had a stage 4 MH (12.5%). These are summarized in Table 1. Sizes of MH ranged from 0.15 to 0.4 disc diameter.

Three hours after surgery, 5 eyes were examined by FD-OCT. Three of these eyes showed comparatively clear images to determine MH closure. The remaining 2 eyes did not show interpretable images because of the media opacity. On the day after surgery (day 1), the macular area could be examined by FD-OCT in 13 eyes, whereas it could not be imaged clearly in 3 eyes because of media opacity: 2 eyes because of corneal haziness and 1 eye because of minimal hyphema. Among 13 eyes examined,